UNIVERSIDADE DA BEIRA INTERIOR
Engenharia

Fault Tolerant DC-DC Converters

Fernando José Figueiredo Bento

Dissertação para obtenção do Grau de Mestre em
Engenharia Eletrotécnica e de Computadores
(2º ciclo de estudos)

Orientador: Prof. Doutor António João Marques Cardoso

Covilhã, junho de 2016

UNIVERSIDADE DA BEIRA INTERIOR
Engineering

Fault Tolerant DC-DC Converters

Fernando José Figueiredo Bento

Dissertation for obtaining the degree of Master of Science in
Electrical and Computer Engineering
(2nd cycle of studies)

Advisor: Prof. Dr. António João Marques Cardoso

Covilhã, June of 2016

Acknowledgments

This work was just possible due to the contribution and effort of many people, that I would like to acknowledge. First of all, I want to thank to all my family, specially my parents, brothers and grandmother, for the support given during this long journey.

I would like to demonstrate my deep gratitude to my Master Dissertation advisor, Prof. Dr. António João Marques Cardoso, for the supervision and for providing workspace and laboratory equipment that allowed me to successfully accomplish this work.

I would like to thank to all my teachers and university colleagues for the knowledge and experiences shared along these five years. Without them, I would not be able to reach this level.

I also wanted to leave a consideration word to all the members of CISE - Electromechatronic Systems Research Centre, in particular to Dr. Jorge Estima and Prof. Dr. Davide Fonseca, that promptly helped me in many technical details of my work.

Thanks to my laboratory colleagues and friends Maria, Saúl, and Waled for the company and help provided throughout this year.

Finally, I want to thank to all my friends, with a special thanks to Serafim and Tiago Machado, for all the advices and company given along my academic career, since I started working on Universidade da Beira Interior.

Resumo

O avanço da tecnologia verificado nos últimos tempos é notório, sobretudo nas cargas utilizadas em nossas casas. Esse avanço trouxe até às nossas habitações novos equipamentos eletrónicos e outras cargas compatíveis com DC, que fazem uma gestão mais eficiente da energia, recorrendo a conversores eletrónicos de potência para esse efeito. Estas cargas têm como denominador comum o facto de necessitarem, em determinado ponto, de retificar para DC a energia AC absorvida da rede elétrica.

Por outro lado, assistiu-se ao crescimento significativo do número de sistemas de micro-geração de energia. A grande maioria destes sistemas produz energia DC.

Estas duas constatações, aliadas à crescente pressão relacionada com a necessidade de sistemas eficientes em termos energéticos, levarão a que, num futuro próximo, redes DC à escala de bairros sejam implementadas, permitindo assim a ligação de instalações de micro-geração a cargas DC, dentro do mesmo bairro, como uma forma de reduzir o número de passos de conversão de energia, bem como as perdas no transporte dessa energia através de redes AC convencionais.

Num futuro em que redes DC serão utilizadas, é essencial a criação de vários níveis de tensão que permitam a ligação dos diferentes tipos de cargas alimentadas a partir de DC. Apenas os conversores eletrónicos DC-DC permitem produzir os diferentes níveis de tensão necessários. A fiabilidade desses conversores torna-se, por isso, num fator de importância extrema na continuidade do fornecimento de energia às cargas a eles ligadas e, ao mesmo tempo, na manutenção da qualidade da energia entregue por parte desses conversores a essas mesmas cargas. Com o aumento da fiabilidade destes conversores em mente, este trabalho aplica uma forma de deteção de falhas por circuito aberto nos semicondutores de potência, aplicável em diversas topologias de conversores DC-DC. Após a deteção de uma falha de circuito aberto em qualquer um dos IGBTs do conversor, são realizadas ações de reconfiguração, que não são do mais que alterações no controlo do conversor que permitirão reduzir os impactos dessa falha, como por exemplo o aumento do *ripple* na corrente. De forma a verificar a efetividade destes métodos, foram efetuados ensaios experimentais, recorrendo a um protótipo do *interleaved DC-DC boost converter* de três fases, ligado a uma carga resistiva.

Palavras-chave

DC@Home, conversores DC-DC, deteção de falhas, tolerância a falhas, fiabilidade.

Abstract

Technology advancement verified in recent times is flagrant, specially in our home appliances. This advancement brought to us new electronic equipment and other DC-compatible appliances with improved capability for energy management, using electronic converters for such purpose. These loads have in common the fact that, at a certain point, they need to transform the AC energy of the grid to DC.

Furthermore, an important increase in the distributed generation of energy has been witnessed. The majority of these systems produce energy in DC.

These two statements, combined with the increased pressure related to the need of energy efficient systems, will certainly trigger, in a near future, the adoption of district-scale DC grids that connect DC generation plants and consumers, in an effort to reduce the number of conversion steps required to deliver power to a DC appliance and, at the same time, limit power losses arising from the energy transportation using conventional AC grids.

In a future where DC grids will be used, several DC voltage levels will be required to allow the connection of the different load profiles that require DC. The inclusion of DC-DC converters will allow the creation of these voltage levels. The reliability of such converters plays a key role, as it ensures service continuity for the DC loads connected to them and, at the same time, preserve the quality of the energy delivered by these converters. With the reliability levels increase as a goal, this work uses an open-circuit fault-diagnostic method suitable for several DC-DC converter topologies. After detecting an open-circuit fault in any of the converter power switches, the control of the converter is re-adapted in order to minimize the adverse impacts of an open-circuit fault, namely the increase of the current ripple. To verify the effectiveness of these strategies, laboratory tests were conducted, using a three-phase interleaved boost converter prototype connected to a resistive load.

Keywords

DC@Home, DC-DC converters, fault detection, fault tolerance, reliability.

Index

List of Figures

List of Tables

List of Acronyms

AC	Alternating Current
BCM	Boundary Conduction Mode
CCM	Continuous Conduction Mode
DC	Direct Current
DCM	Discontinuous Conduction Mode
eV	Electron-Volt
EV	Electric Vehicle
GaN	Gallium Nitrite
IEEE	Institute of Electrical and Electronics Engineers
IGBT	Insulated Gate Bipolar Transistor
LED	Light Emitting Diode
PI	Proportional-Integral
PWM	Pulse-Width Modulation
RPM	Revolutions per minute
Si	Silicon
SiC	Silicon Carbide
VFD	Variable Frequency Drive

Chapter 1

Introduction

The continuous advancement in the technology is a easily perceived reality by all of us. This advancement occurred in a wide variety of fields: in industry, where many manufacturing processes became autonomous; in transportation, with the electric vehicle generalization; in telecommunications, with the spread of optic fibre and super-fast wireless communications; among many others. A majority of such evolution was achieved because of the advancements in the Power Electronics field. Efficient power switches able to deal with significant power densities were just one of the facts that leveraged the advancements in the fields referred above. Recently, the development of smaller and more efficient semiconductors, namely the semiconductors with Wide Bandgap materials (GaN and SiC), promises further developments in this domain.

These deployments make us believe that DC-DC converters might become very useful, in a near future, in medium/high power equipments.

The use of electronic equipment, as well as other DC-compatible loads witnessed a significant growth. Similar trend were followed by the distributed generation systems, that have spread in the last years. These two statements will trigger, with a high degree of certainty, the adoption of DC micro-grids in a near future, connecting distributed generation plants and consumers, with the reduction of the power conversion steps in mind. In a future where those grids will be used, several DC voltage levels will be required, enabling the connection of the several household DC loads. Using DC-DC converters in those grids will enable the use of such voltage levels.

The DC-DC converters applied in those grids will have high reliability levels as requirement, as this is a preponderant factor in the maintenance of the smooth load operation, as well as the converter itself. With the reliability increase in mind, this dissertation aims to contribute to this increase.

Thus, the first chapter will contextualize this dissertation. A state-of-the-art about fault detection and reconfiguration in DC-DC converters will be included, with emphasis on interleaved converters.

The second chapter describes the working principles of the three-phase interleaved DC-DC boost converter, applied in this study, comparing its operation mode under normal circumstances with its operation under faulty conditions.

The strategy used for the open-circuit fault detection is explained in detail in the third chapter. This strategy, that can be used in other DC-DC converter topologies either, analyses the DC bus current, taking into account the changes verified in well-defined timeslots of this signal.

After an open-circuit fault detection in one of the converter IGBTs, the converter control is changed in order to reduce the negative impacts of an open-circuit fault, namely the increase in the current ripple. The fourth chapter explains such reconfiguration process.

To prove the effectiveness of the fault detection and reconfiguration strategies, the fifth chapter presents the simulation results obtained from this converter and corresponding controller when such strategies are used. This simulation takes several cases into account, namely the operation in several converter operating modes, and resilience of the fault diagnostic algo-

rithm to significant load variations.

The following chapter validates the simulation results through an experimental study, performed with the help of a prototype of the converter under analysis. This experimental set-up has similar conditions to those used for simulation purposes.

Finally, the seventh chapter presents a brief analysis of the obtained results and corresponding critical analysis.

1.1 Why is DC so Important?

1.1.1 DC Loads in our Dwellings

Technology is advancing at an astonishing rate. Some of these advancements brought into our dwellings plenty of new equipment that were not part of our daily routine until now. Digital devices such as computers, tablets, smartphones, printers, televisions, and LED illumination achieved large growth rates over the last years, accounting for an important portion of the total energy consumption in our homes. These equipments are DC-powered, which means that their connection to a common socket implies the use of an AC-DC converter in each DC equipment, leading to a significant use of equipment dedicated to power conversion, as well as higher losses in the power conversion process.

Besides these loads, whose supply is made exclusively in DC, there are many others that can be powered either by AC or DC, as for instance heating appliances. According to [1], the loads that fulfil these requirements represented about 50% of the overall energy consumption of a dwelling in the Europe - 27 in the year 2009. Figure 1.1 gives detailed information about the contribution of each appliance to the overall electricity consumption of a dwelling.

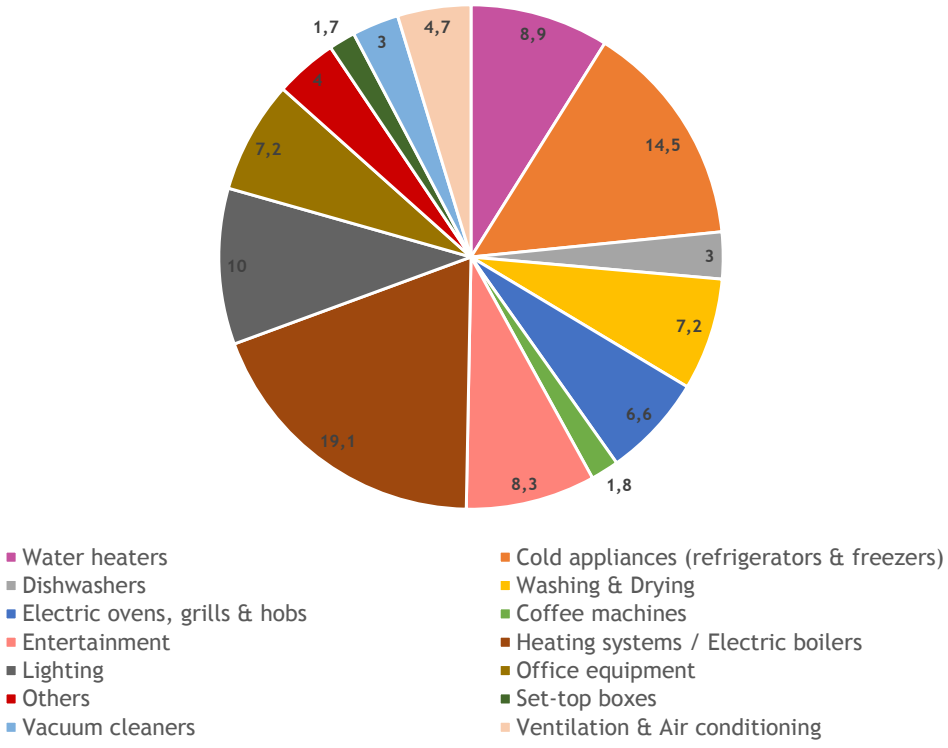

Figure 1.1: Average residential electricity consumption by end-use in Europe - 27. Adapted from [2].

Since then, a growing trend in the energy consumption has been verified, as stated in [3]. This report also concludes that energy consumptions related to small household appliances, where we can frame almost all DC-compatible appliances, has experienced a small increase in the period 2007-2012. That difference is even more significant if we consider the period 2000-2012. In that period, there was an increase of about 40% in the energy consumption related to small household appliances.

Additionally, other changes are being verified in the loads we possess in our dwellings, namely an increasing trend in the use of variable frequency drives (VFDs) in many household large appliances. This VFDs are distinguished by the improvements in the efficiency in those equipments. Air conditioners, washing and drying machines, refrigerators and microwaves are the main targets and, at the same time, the loads that account for an important portion of the energy consumption in a dwelling [3].

The effective rotation speed of an induction machine is given by (1.1), where N is the machine rotation speed, N_s is the synchronous speed and s is the slip.

$$N = N_s \times (1 - s) \tag{1.1}$$

To change N while the machine is running, either N_S or s needs to be changed.

A speed regulation by means of a slip s variation implies the regulation of either the voltage supply level or the rotor resistance. However, these solutions are not the most effective as they present a significant reduction in the machine efficiency. Besides that, some of them present a restrict range of implementation. The use of alternative speed control methods is, therefore, desirable.

The synchronous speed N_s of an induction machine is computed using equation (1.2), where f is the frequency of the power supply and p is the number of pole pairs.

$$N_s = \frac{60 \times f}{p} \tag{1.2}$$

Therefore, the synchronous speed of a machine N_s, in RPM, depends on the power supply frequency f, in Hz, and on the number of pole pairs p, a constructive feature of the machine in analysis that is, in the majority of the cases, impossible or difficult to change. Therefore, the synchronous speed and, hence, the machine rotational speed is directly dependent upon the power supply frequency f. The use of VFDs allows, therefore, a simplified and efficient control of the synchronous speed of those machines, by varying the power supply frequency.

The common arrangement of an VFD, depicted in Figure 1.2, comprises rectification, power factor correction and inversion.

The main reasons that have led to this transform in many of the last generation large appliances are mainly related with speed control, which gets significantly simplified when these structures are used, attaining important gains in terms of energy efficiency. As depicted in Figure 1.3, an air conditioner system controlled by means of a VFD can maintain the compressor running at a constant speed (or close to that). In a traditional system this is not feasible; the compressor can only be turned on or off, which implies higher energy consumption.

A careful analysis of Figure 1.3 allow us to make an important remark: VFDs make use of a DC bus inside the drive. Thus, the long list of DC-compatible loads of our dwellings gets even longer, as VFDs allow the use of DC power supplies. As these structures are starting to be applied

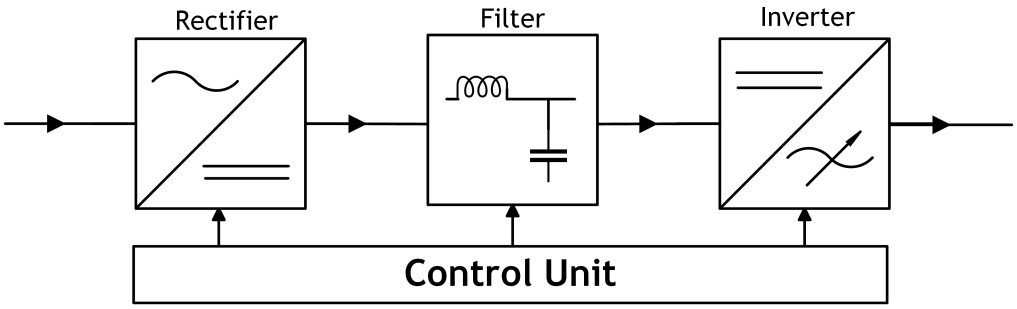

Figure 1.2: Simplified structure of an electronic frequency regulator. Adapted from [4].

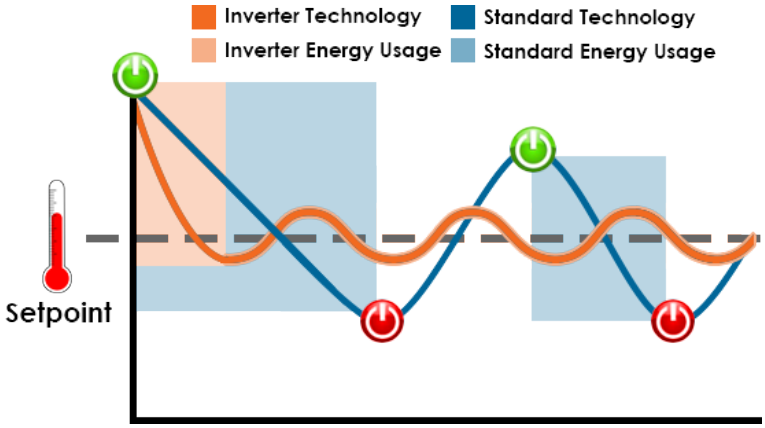

Figure 1.3: Behaviour of a traditional air conditioner vs. air conditioner with VFD. Extracted from [5].

by many of the most important manufacturers of household large appliances, it is expected that other companies will follow the same steps. Therefore, a generalization in the use of VFDs in the large appliances of our dwellings is expected.

Nevertheless, more changes are being witnessed in the way our energy is consumed in our dwellings. The electric vehicle (EV), facing a fast expansion phase, is expected to represent a huge amount of energy consumption in our dwellings because of its recharging process. This process requires the connection into a common socket. However, and like any other energy storage system made from batteries or super-capacitors, an AC-DC conversion is required to supply the batteries of the EV [6].

1.1.2 Domestic Microgeneration Evolution

Deep transformations occurred in the type of loads that we possess in our dwellings. Besides that, the importance of each type of load in the overall energy consumption of a dwelling changed significantly (small appliances increased their importance in the overall energy consumption of a dwelling and, on the other hand, large appliances reduced their significance). Nevertheless, the changes were not limited to the way energy is consumed in our dwellings. Big changes were also stated in the way energy is produced. An increase in the number of distributed generation systems was stated, encouraged by environmentally friendly policies. Figure 1.4 gives a general view about the growth in the installed capacity related with microgeneration systems in Portugal between 2008 and 2011. It should be noted that a small percentage of the installed power refers to other microgeneration systems that do not belong to domestic systems.

These systems make use of some renewable sources of energy and are usually constituted

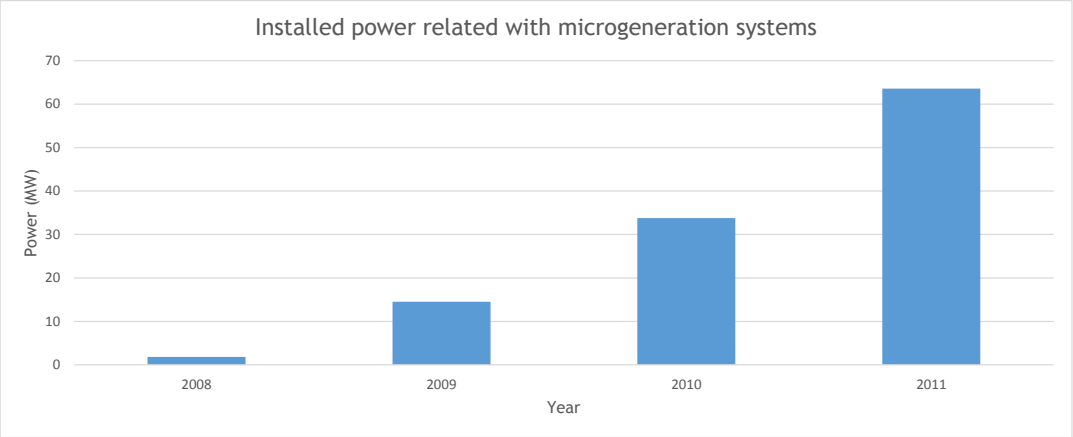

Figure 1.4: Total installed power related with microgeneration systems. Adapted from [7].

by photovoltaic modules and/or small wind turbines. The majority of these systems operate in DC [8, 9]. Moreover, most of the energy produced by these systems are currently injected into the grid, which implies the use of DC-AC converters to realize the interface between microgeneration systems and the grid.

1.2 Finding the Best Ways to Save Energy

The energy conversion processes made by means of power electronic converters suffer, in general, cuts in the conversion efficiency as the number of conversion steps increases. As the converters used for the tasks referred above usually comprises several conversion steps (the most common are transformation, rectification/inversion and power factor correction), they present fairly low efficiencies, as stated in [10].

1.2.1 Alternative Grid Architectures

Taking into account all these evidences (the growth of the DC-compatible home appliances, the increasing number of microgeneration plants and the poor performance of power rectifiers and inverters), it is mandatory to find other options. Reducing the number of power conversion stages would significantly reduce the required equipment, leading to lower power losses in the conversion process. Such reduction could be reached by adopting small-scale DC distribution grids applied at the residential level. This way, microgeneration plants and DC-compatible loads could be connected each other, using DC-DC converters as the interface structure between microgeneration facilities and loads. As DC-DC converters involve a reduced number of components and, hence, of conversion steps, these converters present, generally, higher efficiencies when compared with AC-DC or DC-AC converters. If we consider again the VFD, whose architecture currently implemented in many household appliances is depicted in Figure 1.2, and transpose it to a solution where DC grids are implemented, the result will be similar to that presented in Figure 1.5. As seen in Figure 1.5, the rectification process is eliminated when a DC supply is used, which is why DC-DC converters may present a solution with higher efficiency.

Similarly, we can generalize the DC grid concept to an entire building. Figure 1.6 establishes a comparison between the *status quo* of the energy distribution system in a dwelling (Figure

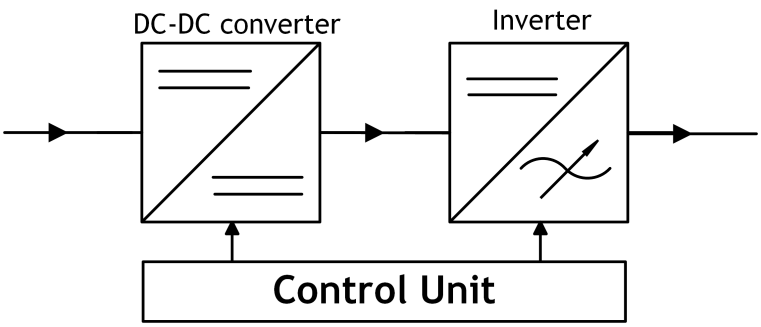

Figure 1.5: Simplified structure of an electronic frequency regulator supplied with DC.

1.6(a)) and a feasible alternative (Figure 1.6(b)). It should be mentioned that a DC power distribution system containing an energy storage system, similar to that presented in Figure 1.6(b), may connect the energy storage devices (batteries or super-capacitors) to the DC bus without resorting to DC-DC converters, depending on the system specifications. When those converters are dispensed, the losses related to the power transfer between energy storage devices and DC bus are fairly low (0% to 2% losses). However, slightly higher losses should be expected if power converters are used in the process.

Several case studies proposed alternative embodiments to the conventional power distribution system at the residential energy distribution level, establishing a comparison with the actual systems [12–15]. Despite the small differences between the proposed models, all of them showed that it is possible to significantly reduce the energy losses related to conversion from AC to DC if such variations were implemented. The systems applied in those studies have a high resemblance degree with the one presented in Figure 1.6(b), with the replacement of AC-DC and DC-AC converters for DC-DC converters as a common denominator.

Alongside with this studies, further initiatives are being developed by international institutions, namely IEEE. One of them, called "*DC in the Home*" [16], intends to appoint and quantify the energy losses resulting from the state-of-the-art power electronic converters and, at the same time, establish which steps should be considered in the implementation of this alternative. A similar initiative, called "*Indian Low Voltage DC Forum*" [17], takes on similar aims. It intends to accomplish real environment tests that prove the effectiveness of these solutions. At the same time, it also aims to contribute on making informed decisions about the most effective way to deploy low an medium DC voltage systems.

DC-DC converters will be, therefore, required in DC grids to provide several DC voltage levels that satisfy the requirements of the different loads. This presents a presage about the relevance that these converters may play in the energy conversion for household systems and many other applications.

Other important measures will be required to enable the full deployment of the solutions proposed above. Besides efficient and reliable DC-DC converters, it is also important to develop several auxiliary systems, as for instance protection systems compatible with DC. Most of the protection technologies currently available for AC systems are not compatible with DC. Circuit breakers and power electronic protection devices are two examples of protection technologies. These protections will be needed for application in sockets, switches, energy storage systems, Power Electronic converters, and so on. Researchers are starting to develop some solutions related to this topic, specially circuit breakers [18, 19], and DC sockets and switches [20–22].

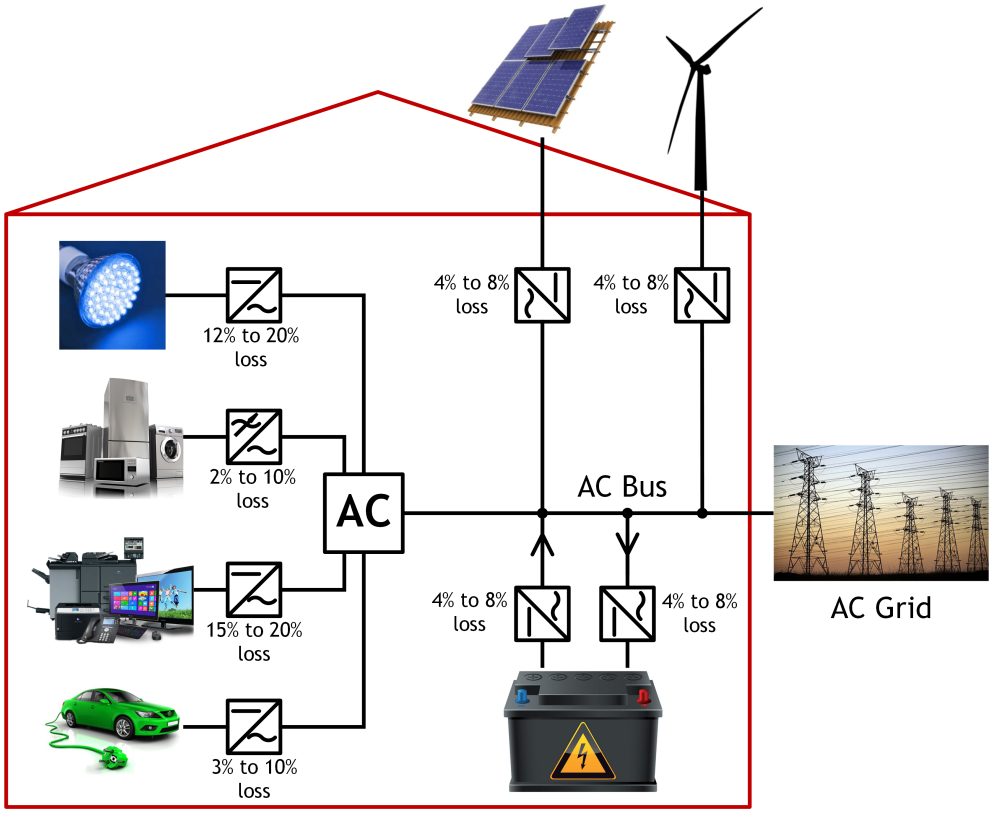

(a)

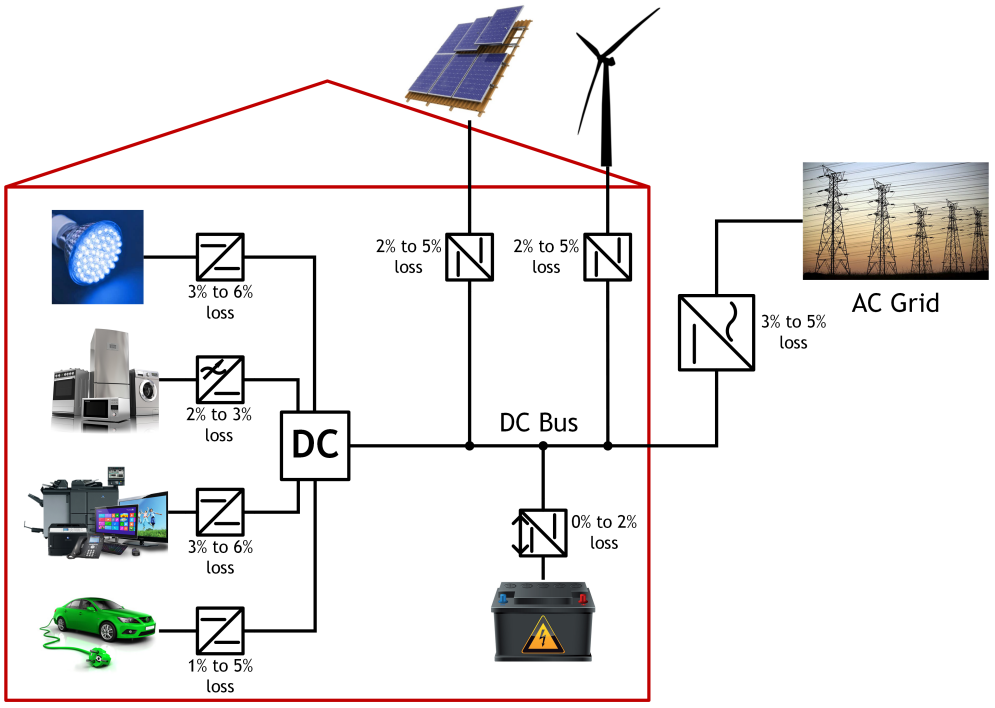

(b)

Figure 1.6: Power distribution system in a dwelling: (a) Typical structure; (b) Proposed structure. Adapted from [11].

1.2.2 Last Generation Semiconductors in the State-of-the-Art Power Converters

Other ways to reduce the AC-DC energy conversion losses, or vice-versa, could be also used to make a quicker transition to a solution with efficiency improvements.

The developments achieved in the Power Electronics field in the last few years were significant, with the deployment of faster and more efficient semiconductors, as for instance the Wide Bandgap semiconductors of GaN and SiC. The denomination given to these materials are related to the higher electronic bandgap between electronic levels or, in other words, the gap between the valence band and the conduction band. Table 1.1 compares the bandgap between the most common semiconductor materials [23].

Table 1.1: Semiconductor materials.

Material	Bandgap Energy (in eV)
Si	1.1
SiC	3.3
GaN	3.4

The features of these materials can overcome the main constraints of Si devices, being able to block high voltage levels, operate at high-temperature conditions and high switching frequencies. These features allow, therefore, the power converters performance enhancement when these devices are used. Further benefits can be attained when using Wide Bandgap devices, as for instance, reduction in the power converter materials (bulky cooling systems can be reduced due to the lower switching losses; passive components can be reduced due to higher switching frequencies) [24].

Both GaN and SiC present high performances, though GaN offers better theoretical results in terms of high-frequency and high-voltage operation. However, better quality substrates are available for SiC devices, putting SiC in a better position to manufacture power switches in the high-voltages segment and GaN in the low/medium-voltages. Nevertheless, plenty of work still needs to be developed to fully exploit the benefits of these materials, starting with improvements in the substrates quality and matured manufacturing processes [24].

Thus, the application of the last generation semiconductors in the state-of-the-art power converter topologies (AC-DC and DC-AC) would reduce the losses related to energy conversion processes. However, this solution would not be the most interesting one as it would not reduce significantly the bill of material of those converters and, hence, the potential reduction in the converter losses would not be fully exploited.

1.3 Loads Susceptibility to Voltage/Current Fluctuations

Many of the DC-compatible household appliances, specially electronic loads (e.g. computers, printers, televisions, smartphones, LED lighting, etc.) are very sensitive to voltage and current fluctuations. From the point of view of the solutions proposed in [12–15], where the interface between grid and these loads are performed by means of DC-DC converters, the adoption of low cost DC-DC converters able to ensure high efficiency, high reliability and low output current ripple to such loads is crucial.

Keeping high reliability levels in converters supplying energy to these loads has a major im-

portance. Such levels should remain as high as possible, even if any component of the converter becomes faulty. A fault in a converter component means, in most cases, lower power quality levels that endangers the load connected to the converter. Once connected to a faulty converter, those loads experience overheating, leading to their early ageing or, in some cases, to complete stoppage of the load operation, depending on the depth and duration of the fault [25, 26].

A large amount of household appliances use batteries, whereby the same negative effects could be expected in the battery's lifespan. As show in [27], the ripple of the voltage applied to a battery during the charging process should not surpass 0.5% of the DC voltage, under normal conditions. The same effects can be expected in the converter output capacitor when the current crossing the capacitor present high ripple levels [28].

Interleaved DC-DC converters are one of the topologies that fulfil the above requirements. The input current of the converter is split into n phases, with each phase current shifted by $2\pi/n\ rad$ between subsequent phases. In fact, great benefits are attained with this approach, namely ripple reduction in both input and output current and lower per phase current rates [29]. Besides that, this is a multi-phase converter, allowing the converter operation continuity, even if one or more power switches stops working (fault isolation remains as a fundamental condition for continued operation).

1.4 Previous Studies in the Domain of DC-DC Converters

1.4.1 Most Common Components Prone to Failures

Power converters, like many other equipment, can suffer from the occurrence of failures. Inside these converters, several components might be the cause of faults. Nevertheless, semiconductors and capacitors are the most common source of faults in power converters. Within semiconductor faults, that can be classified into open-circuit faults and short-circuit faults, the open-circuit faults are generally caused by gate drivers failures, wire lifting or soldering break [30, 31].

Therefore, the detection of such failures is essential. The adoption of control strategies that reduce the impact of such faults in the load and other converter components is even more important. Some work on short-circuit faults in DC-DC converters have already been made [32–34]. Although detection of such faults can be achieved through software, several protection measures against this kind of failures are already implemented in the state-of-the-art DC-DC converters, namely physical protection devices that isolate the fault in a shorter time when compared with similar protection strategies implemented using software. Short-circuit faults require a fast response time that allows the fault isolation, thus minimizing damages in the converter and/or the load connected to it. Generally, software protection does not achieve the quickness needed to the minimization of adverse impacts of these faults. Additionally, these faults present a big barrier or even inability to the converter operation continuity.

On the other hand, open-circuit faults are not so damaging as short-circuit faults. In the case of the converter under study, the energy supplied to the load is sustained as the rest of the healthy phases keep conducting. Nevertheless, this energy is supplied to the load under worst conditions (more ripple and lower power factor), which is why many of the research effort focuses on open-circuit faults. The current ripple in the input side of the converter also suffers an important growth.

1.4.2 State-of-the-Art on Open-Circuit Fault Detection and Reconfiguration

Several open-circuit fault detection methods applied to different kinds of DC-DC converters have been proposed by several authors. Different strategies were applied to achieve the open-circuit fault detection: use of Kalman filters [35], measurement of the transformer primary voltage and its behaviour analysis [36], comparison of the duty cycle with the inductor current slope [37], analysis of the current waveform and its variation in different points of the converter [33, 38–41], capacitors voltage monitoring [42, 43], magnetic near-field waveforms monitoring [44], use of a state estimation approach [45] or the magnetic components voltage waveforms [46]. These works were performed for different topologies of DC-DC converters. Some of them are restricted to specific topologies of DC-DC converters; some fault detection algorithms are just concerned about some operating points of such converters, as for instance converters switching under either zero voltage or zero current conditions or just under discontinuous conduction mode (DCM) or continuous conduction mode (CCM); others have a broad spectrum of action, but are very complicated or have long fault detection times.

Although fault detection assumes a major importance, converter reconfiguration after a fault also plays an important role, as it allows operation continuity with acceptable quality levels. It is relevant to deploy reconfiguration strategies able to maintain the fault-tolerant converter hardware structure as simple as possible, considering a fault-tolerant converter without any additional hardware the most attractive solution. Load and the output capacitor are the most benefited components, as similar levels of pre-fault power quality are achieved, even after the open-circuit fault. Nevertheless, the healthy IGBTs are subjected to slightly higher current ratings and, therefore, higher heating as a consequence of increased conduction losses. For that reason, special careful must be taken when a faulty converter operates at its full load, or close to that operating condition.

To address these concerns, this dissertation applies a fast open-circuit fault detection algorithm and reconfiguration strategy after a fault in any of the converter phases. The fault detection algorithm follows the principle used in [41], with the implementation of such principle in multi-phase DC-DC converters. In [33], an identical approach is applied to single-switch DC-DC converters using a state-machine.

After detecting a fault in any of the IGBTs, the PWM generator changes the features of the PWM signals in order to re-organize the converter operation, without any additional hardware devices.

Chapter 2

Converter Operation

This chapter provides detailed information about the operating principles of the converter used in this work. The control strategy applied in the converter is also explained. After that, both normal and faulty operation are compared. Based on this comparison, strategies suitable for fault detection can be discussed.

2.1 Converter Control Strategy

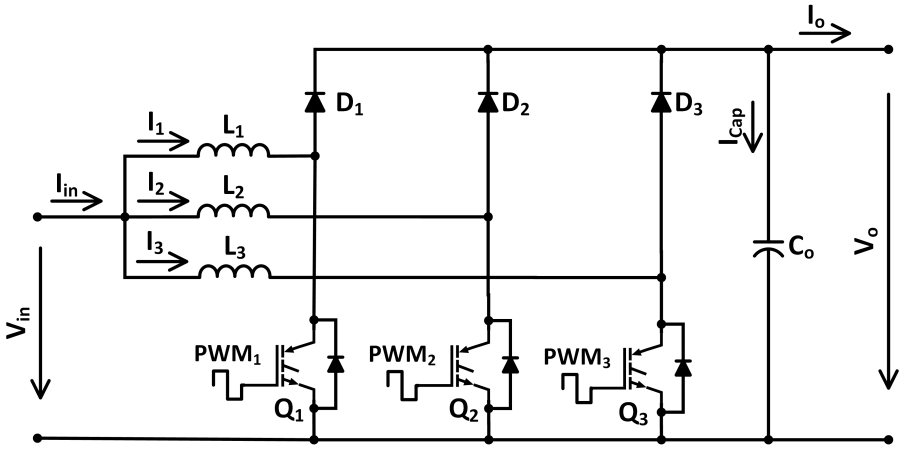

Figure 2.1: Three-phase interleaved DC-DC boost converter.

Figure 2.1 depicts the three-phase interleaved boost converter used for this study. As this converter is composed of three phases, a phase-shift of $2\pi/3\ rad$ between each phase current is applied to produce a pattern similar to a three-phase current system. Depending on the conduction pattern of each phase inductor, this converter may operate in three distinct modes: discontinuous conduction mode (DCM), boundary conduction mode (BCM) or continuous conduction mode (CCM). Each operating mode has its advantages and disadvantages. One of the major differences between DCM and CCM is the fact that conduction losses are dominant in DCM, while switching losses are the most important source of losses in a converter operating in CCM. Nevertheless, some authors made deeper analysis on the efficiency of these converters. One of those studies presented the pros and cons of both DCM and BCM [47].

Switched power converters usually require complex control strategies. Several control strategies are available, with different complexity degrees. For lower voltage step-up ratios and light-load conditions, a simple voltage controller might be applied to effectively control the converter, with reasonable results. In these conditions, a single PI controller whose input is the output voltage error, given by the difference between V_{ref} and V_o, can perform the task with success. This is due to the fact that, under these conditions, the converter generally operates in DCM, which allows a stable converter operation, without significant imbalance between converter phases.

Converter operation in CCM brings some problems to the voltage control strategy, causing serious current imbalance between converter phases related to small differences between physical components, especially inductors, and mismatch in the duty cycles applied to each power switch. This instability is harmful for the power switches due to unequal current sharing between converter phases that cause thermal stress to the phase(s) with current surplus. Hence, it is desirable to apply another control strategy able to manage the converter operation with good results in a wider range. An average current control strategy can successfully solve most of these problems. In this strategy, two control loops are used: a voltage regulator and a current regulator. The voltage control loop is the external loop and adjusts the converter output voltage using a PI controller. This regulator uses a small bandwidth to avoid the negative effects of the input ripple in the converter output voltage. The output of this loop, along with the sampled values of the input voltage V_{in} and the square value of the RMS voltage V_{in}, are going to define the value of the reference current I_{ref}. Before using it in the controller, the amplitude of the input voltage V_{in} signal is reduced, by applying a reduction factor. This reference signal, introduced in the current control loop, has the same shape and phase of the input voltage signal. This loop, called the inner loop, is responsible for correcting the current error, defined as the difference between the reference current I_{ref} and the effective converter input current I_{in}. Besides that, this loop has a wide bandwidth that enables a fast response from this regulator, allowing it to track fast oscillations in the current reference signal [48–50]. This approach is commonly used in converters dedicated to power-factor correction.

However, this work took another approach. Unlike other works that focus the control of interleaved DC-DC converters for power-factor correction effects, this work focuses on applications where the DC-DC converter input is a stabilized DC voltage and, at the same time, uses simple loads to perform the laboratory tests. So, instead of using the original version of V_{in}, this signal is filtered to limit the oscillations of V_{in} seen by the controller, using a discrete low pass filter for that purpose. Figure 2.2 shows the blocks used in the implementation of such control strategy.

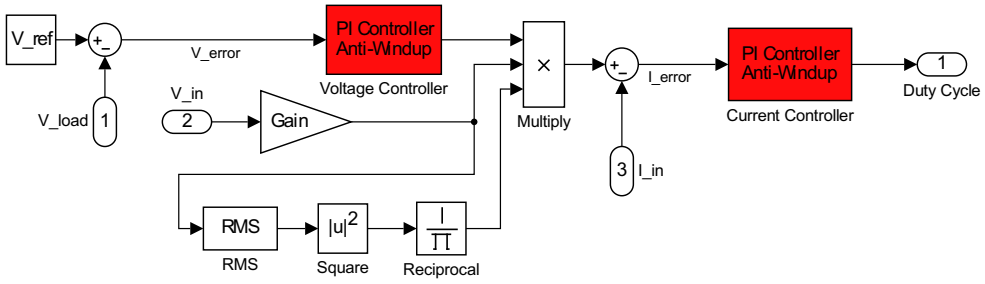

Figure 2.2: Average current controller used in the interleaved DC-DC boost converter.

This control strategy presents a wide applicability range. It can effectively control the interleaved DC-DC boost converter in both DCM and CCM modes. Likewise, it can also control many other switching power converter topologies. Similar strategies based on the same principle have also been developed to overcome some issues that may arise. Interleaved DC-DC converters may show some imbalance between phases, even with this control strategy. To avoid this, all inductor currents are compared between them and, in case of imbalance, an adjustment in the duty ratio is introduced [49].

2.2 Circuit Behaviour under Normal Operation

The converter input current comprises the sum of each phase current (2.1).

$$I_{in} = I_1 + I_2 + I_3 \tag{2.1}$$

Each converter phase possesses identical components, whereby a balance between phases is expected. However, small differences between phase inductances or parasitic resistances may impair this balance [51]. Therefore, the range of values assumed for each phase current will be similar. With this in mind, and considering the fact that I_{in} is commonly used for control and safety purposes, this signal can be one of the best options to monitor an abnormal behaviour of the converter.

Taking into account the identical nature between phases, an analysis will be performed for just one converter phase. When the power switch is conducting, the voltage across the inductor equals the input voltage. On the other hand, the current crossing the switch is equal to the current crossing the inductor. Therefore, the derivative of the inductor current will be given by (2.2).

$$\frac{dI_L}{dt} = \frac{V_{in}}{L} \tag{2.2}$$

This means that the slope of the current crossing the inductor is constant and positive, increasing linearly while the switch is on.

Meanwhile, when the switch is off, no current flows through it. The voltage across the inductor, given by the difference between the source and load voltages, is negative as the load voltage is higher than the source voltage. Therefore, the derivative of the current flowing through the inductor is given by (2.3).

$$\frac{dI_L}{dt} = \frac{V_{in} - V_{out}}{L} \tag{2.3}$$

Hence, the current crossing the inductor during this time period will decrease linearly after the switch turn-off, possibly reaching zero, depending on the converter operating mode. The behaviour of these variables is depicted in Figure 2.3.

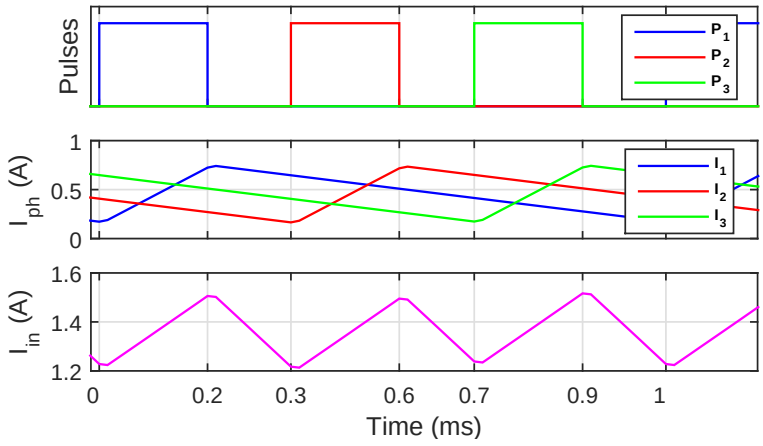

Figure 2.3: Operation of the converter under normal conditions.

2.3 Circuit Behaviour under Faulty Operation

After an open-circuit fault in a power switch, no current will flow through it, precluding any energy flow across the phase associated with that IGBT. Thus, only (2.3) will be verified, meaning that after a fault, the phase current will decrease linearly, reaching zero phase current soon. The frequency of the input current ripple decreases, resulting in an increase in the current ripple in both the input and output of the converter. Figure 2.4 shows a switching pattern with a power switch open-circuit fault in phase 1 at $t = 0.1\ ms$.

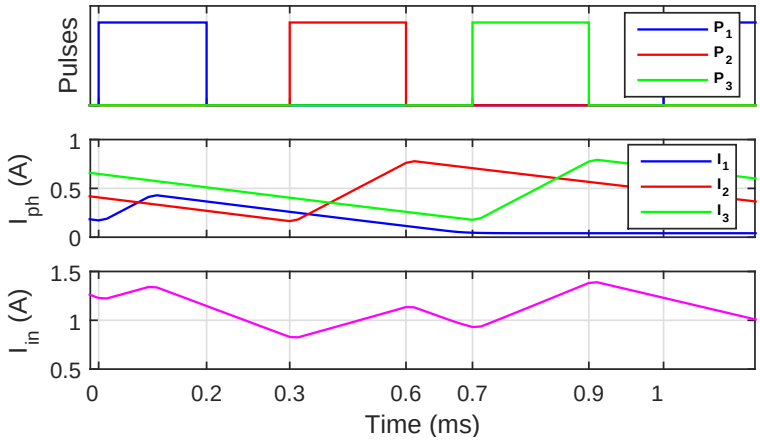

Figure 2.4: Operation of the converter after an open-circuit fault in the power switch of phase 1 at $t = 0.1\ ms$.

As expected, the phase current starts to decrease linearly until reaching zero. This behaviour is usually reflected in the waveform of I_{in}. When it happens, I_{in} decreases until the switch related to the next phase starts conducting. However, it does not occur every time, because the relation between the duty ratio D of the PWM applied to the IGBTs and converter operation mode might determine the maintenance of the increasing trend of I_{in}. Such behaviour occurs when $D > 2/3$ or $1/3 < D < 2/3$ and the converter operates at DCM.

The duty ratio D, along with D_M, are responsible to determine the converter step-up ratio. D_M can be defined as time wherein the phase current is different from zero. In both BCM and CCM D_M is equal to 1, because the phase current never reaches zero. Hence, the converter voltage gain is given by (2.4) [38].

$$\frac{V_{out}}{V_{in}} = \frac{D_M}{D_M - D} \tag{2.4}$$

Therefore, the control structure comprising fault diagnosis and converter reconfiguration has to be applied. The main functions of each block will be detailed in the next chapters.

Chapter 3

Fault Diagnosis

As mentioned in Chapter 2, the converter input current I_{in} contains important information that can be used for fault detection purposes. Fault detection can be achieved by acquiring and comparing the values of I_{in} in different and well-defined moments. The pulses used to trigger each power switch are easily available from the control structure, making them a good choice to define those moments. Using I_{in} as the control variable and the PWM signals together, a trivial solution consisting on the comparison of I_{in} in the rising edge of the PWM signal related to that phase, and the corresponding falling edge can be used in this converter, similarly to what is suggested in [41].

An identical approach is used in [33], where the inductor current slope sign is used to detect a fault (open-circuit or short-circuit faults). As depicted in Figure 2.3, I_{in} increases after the switch turn-on, and will remain increasing until the next falling edge, that can belong to any control signal. To take this into account, the values of I_{in} in the rising edge will be compared with the values in the first falling edge of any of the command signals, making this verification step independent of the duty cycle D. The presence of an open-circuit fault can be easily analysed by subtracting the last value of I_{in} saved in the sample and hold block with the last value from the stack: if the difference is positive (I_{in} increases in the time period under analysis), it means that the power switch associated with that phase is healthy; otherwise I_{in} decreases and an open-circuit fault has occurred in the power switch of that phase. A similar approach can be used to detect also short-circuit faults, taking into account different time intervals. Compared with other open-circuit fault detection algorithms, this reduces the fault detection time. This reduction is especially significant when the converter operates with $1/3 < D < 2/3$. On the other hand, this fault detection algorithm is unable to detect faults when the duty cycle $D > 2/3$ or the duty cycle D is $1/3 < D < 2/3$ and the converter operates at DCM. Within the subject of this work, these operating points are not applied because of their low interest in terms of converter efficiency.

To improve the fault detection effectiveness, a first-order high-pass filter is added to process the I_{in} signal. With this filter, fault detection capability gets enhanced, with improvements on fault detection under harsh converter operation, as for instance load transients. A gain is introduced in the filtered signal to amplify it and give a cleaner view of the signal variations. The basic structure of the fault detection block is presented in Figure 3.1.

The main blocks composing this unit are the stack, the sample and hold, the high-pass filter, the S-R flip-flop and the edge detectors. The working principle is simple: when a rising edge is detected in the PWM signal, the filtered signal of I_{in} is pushed into the stack block. When a falling edge in any of the PWM signals is detected, the filtered signal of I_{in} is stored in the sample and hold block, being instantaneously sent to the block output. At the same time, the last value in the stack is popped, so the values of I_{in} related to the same switching period can be correctly compared. The S-R flip-flop ensures that only falling edges subsequent to the rising edge in analysis are taken into account.

With this configuration, the block compares the values of I_{in} in the rising edge of the PWM signal and the subsequent falling edge of any of the three control signals, allowing the correct

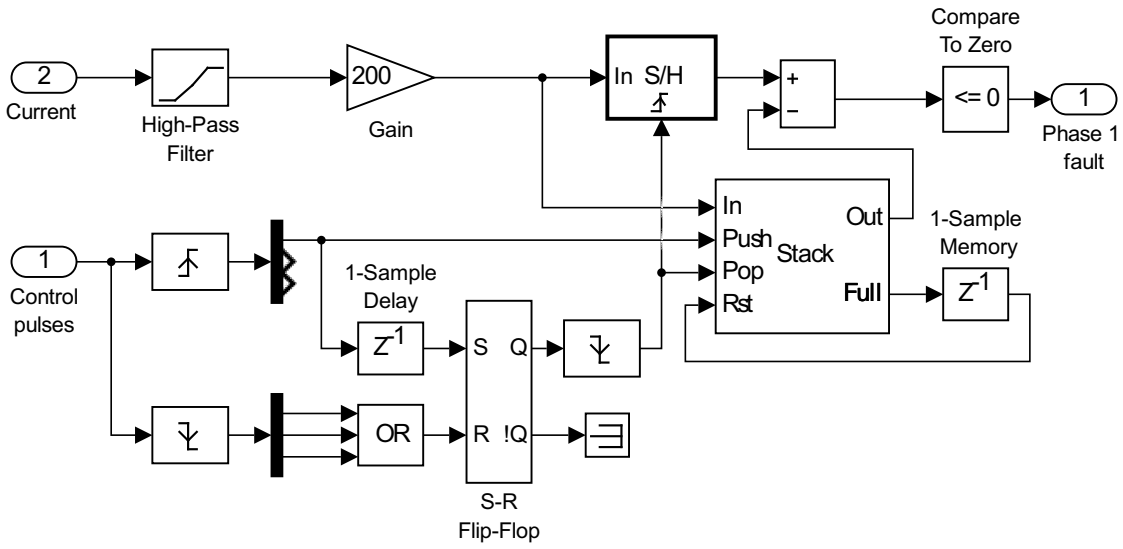

Figure 3.1: Basic structure of the fault detection block.

detection for a wide range of duty cycle values. Figure 3.2 illustrates the sampling moments of I_{in} for different values of D.

However, some issues may arise when this sampling strategy is used for the converter operation with values of D near or equal to $1/3$ and $2/3$. For such duty cycle values, the falling and rising edges of the PWM signals are very close to one another's and the power switches change of state almost simultaneously. In these conditions, the ripple of I_{in} is minimum, making the fault detection process much more complex. In addition, the non-ideal behaviour of the converter components, verified in any practical implementation, also impacts the fault detection. Under these circumstances, I_{in} maintains its descending trend for a few moments after the rising edge of the PWM signal that triggers the IGBT related to the phase under analysis. To overcome this issue, a small delay is applied to the signal that triggers the Push into stack when two edges are close to one another. The delay depends on the switching frequency f_s, duty cycle D and sampling time of the controller T_s. This time delay increases as the time distance between both shortens. The fault detection block requires a few more components to correctly apply the delay, when needed. Hence, a delay block and a function block, responsible to create the expression that computes the number of samples of the delay, are added. Figure 3.3 displays the fault detection block with capability to change the moment for pushing the value of I_{in} into the stack when D approaches $1/3$.

When D approaches $1/3$, the stack block saves the processed values of I_{in} in two moments: the first occurs in the rising edge of the PWM signal; the second appears after the PWM rising edge and represents a delayed version of the last verified falling edge. Figure 3.4 shows an example where D is almost $1/3$. There, two pulses are shown, representing the moments when I_{in} signal is pushed into the stack. In this case, only the second value of the sampled signal will be used for comparison effects, leaving any other data in the stack until its deletion. The second pulse intends to eliminate the false fault detection phenomena arising from non-ideal behaviour of the converter, that is not presented in Figure 3.4.

The fault detection process explained above applies for one converter phase. Some resources used for this purpose have to be replicated in order to have fault detection in all three phases; blocks with the same results are shared between all converter phases.

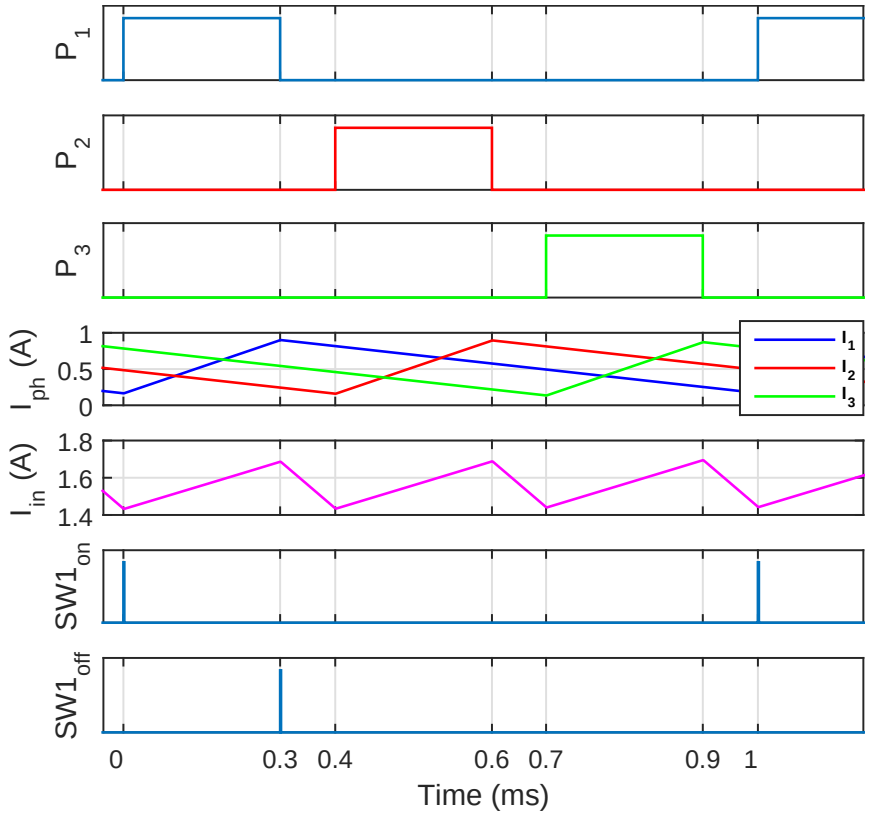

(a)

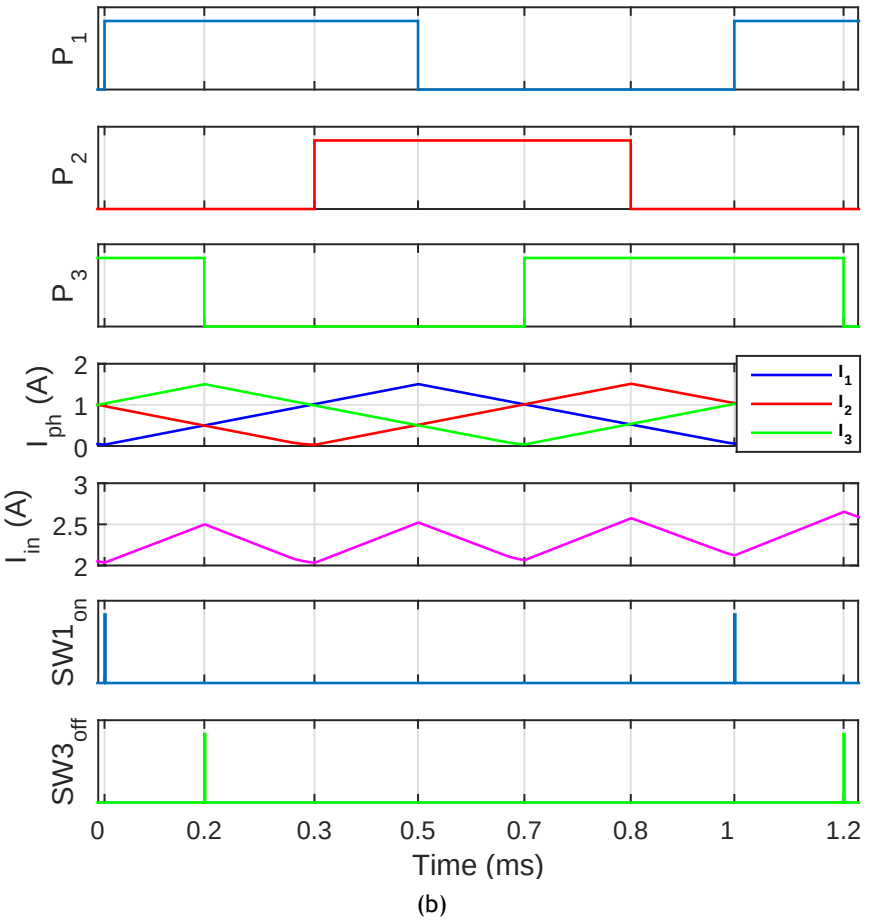

(b)

Figure 3.2: PWM pulses, Phase currents, Converter input current, Push into stack and Pop from stack commands for: (a) $D < 1/3$; (b) $1/3 < D < 2/3$.

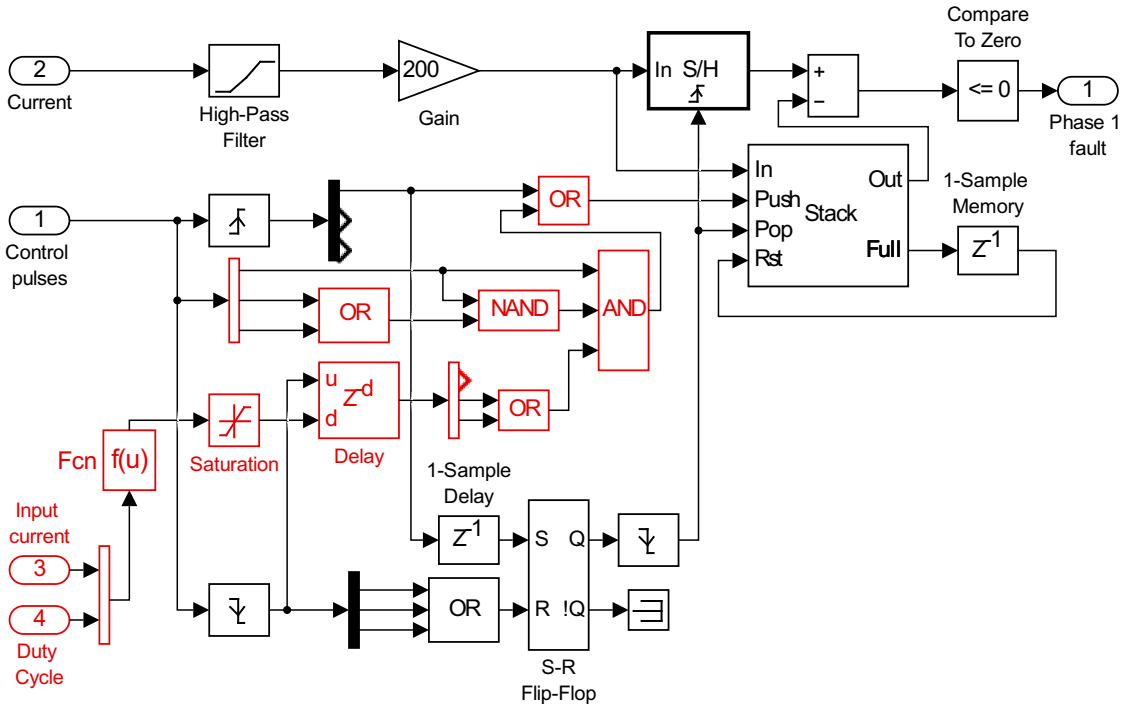

Figure 3.3: Fault detection block with delay capability. The components added to the block are highlighted in red.

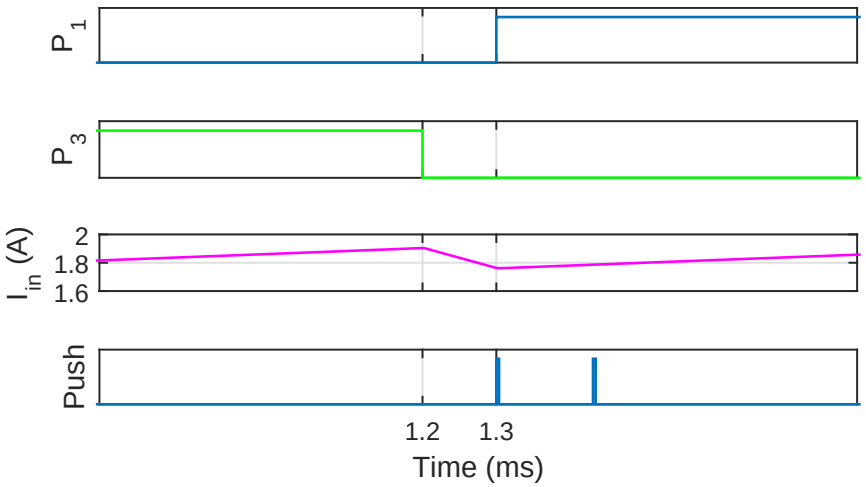

Figure 3.4: Pulses that control the push into stack of I_{in}.

Chapter 4

Converter Reconfiguration After an Open-Circuit Fault

As stated in Chapter 1, it is essential to maintain the good operation of a DC-DC converter, even after an open-circuit fault. It was also verified that a converter whose power switches present open-circuit faults can still deliver power to the load, but under degraded conditions. The most visible effects are the higher fluctuations in the input current I_{in} and output capacitor current I_{Cap}. Higher current variations in this capacitor are experienced to compensate the loss of one converter phase. As a result, the converter capacitor will be highly stressed, with its possible loss. Remedial actions to reduce the impact of open-circuit faults are, therefore, mandatory.

In the reconfiguration strategy used in [52], with other authors working on multi-phase DC-DC converters suggesting the use of such strategy [34, 37, 38], the converter operation is adjusted according to load requirements or in case of power switches failures. After an open-circuit fault in one or more power switches, the PWM signals phase-shift are adjusted according to the number of healthy phases. In the case of the three-phase interleaved boost converter, the phase-shift between PWM signals associated with healthy phases would be changed from $2\pi/3\ rad$ to $\pi\ rad$ after an open-circuit fault; the principle is to change the control strategy from a three-phase converter to a two-phase converter while the converter is online. The same principle is applied in this work for the converter reconfiguration. This action reduces, in general, the current ripple after a fault, but does not allow the converter to reach the level of ripple verified in the original state of the converter. Therefore, additional actions can be taken to reduce the ripple even more.

The current variation on each converter phase, consisting on the difference between the peak values of the waveform, can be obtained using (4.1) [38]:

$$I_M = \frac{V_{in} \times D \times T}{L} = \frac{V_{in} \times D}{f_s \times L} \tag{4.1}$$

From (4.1), it can be easily deduced that the phase current ripple depends on the input voltage V_{in}, duty cycle D, switching frequency f_s and phase inductance L. After an open-circuit fault, I_{in} ripple frequency decreases from $3f_s$ to f_s, resulting in increased current oscillation, in accordance to (4.1). All these parameters, except D and f_s, are fixed or cannot be changed to maintain specific ripple levels. On the other hand, D is used to define the converter step-up ratio, making its use for ripple reduction effects infeasible. Hence, switching frequency f_s can be used, under fault conditions, to minimize current ripple in both the input and output of the converter. Some authors have already developed work related with frequency modulation in DC-DC converters drivers [53–55], but not with fault tolerance purposes. Others have worked with frequency modulation for fault tolerant converters, but for different topologies [37], applying just this reconfiguration strategy. Thus, a control consisting on a combination of adaptive phase-shift and frequency modulation can perform the reconfiguration task with good results.

Here, the idea is to adapt the phase-shift between PWM signals and, at the same time, increase the switching frequency f_s after a fault. To implement such strategy, the block from

Figure 4.1 is used. The most important components are the PWM generator and the phase-shift corrector.

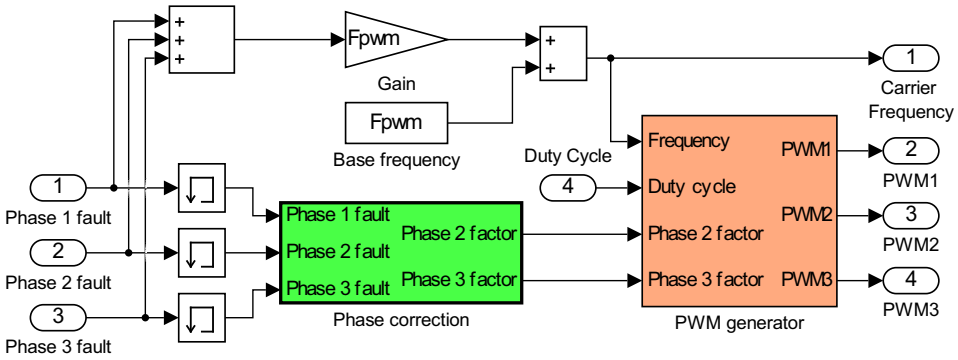

Figure 4.1: Reconfiguration block.

4.1 Phase Correction Component

The phase-shift corrector contains a combinational logic circuit. In the simulation environment, each signal introduced in this component is delayed by one sampling period to avoid algebraic loop errors. According to the information given to this block about the presence and location of faulty phases, the outputs will change the values sent to the PWM generator. Table 4.1 summarizes the possible fault combinations and the corresponding phase-shift between PWM signals. The applied shift takes the PWM signal for phase 1 as reference. In this table, '-' denote the **do not care** state. In other words, the phase-shift may remain unchanged if a transition to that state is verified. For the sake of simplicity, the block was configured with default values (a phase-shift of $1/3T$ for phase 2 and a phase-shift of $2/3T$ for phase 3, where T denotes the PWM signals period).

Table 4.1: Possible fault combinations and their corresponding phase-shifts in the time domain.

States			**Phase shift ($x \times T$)**	
Ph.1 fault	Ph.2 fault	Ph.3 fault	Ph.2 shift	Ph.3 shift
0	0	0	$1/3$	$2/3$
0	0	1	$1/2$	$2/3$
0	1	0	$1/3$	$1/2$
0	1	1	-	-
1	0	0	$1/3$	$5/6$
1	0	1	-	-
1	1	0	-	-
1	1	1	-	-

Generally speaking, this component applies a phase-shift of $1/2T$ to the PWM signal related to the second healthy power switch. To exemplify, let us consider the following example: after an open-circuit fault in Q1, Q2 and Q3 hold their operation; thus, a phase-shift of $1/2T$ between PWM2 and PWM3 has to be applied. To avoid using three output variables in this block, the phase-shift of PWM2 remains unchanged, while PWM3 phase-shift is increased from $2/3T$ to $5/6T$. Figure 4.2 depicts such variation in the PWM signals after the occurrence of an open-

circuit fault. Signals with same colours refer to the same converter phase. PWM1 is disabled after the fault and, as expected, the other two PWM signals are reconfigured instantaneously.

4.2 PWM Generation Component

This component generates PWM signals for all the three converter IGBTs. To ensure the capabilities of fault tolerance, carrier frequency and phase-shift are introduced as inputs in the block to allow these reconfiguration capabilities. PWM signals are produced by a triangular carrier, generated with the aid of two discrete integrators and one look-up table.

The carrier frequency assumes predefined discrete values. Under normal operation conditions, switching frequency f_s remains unchanged along the converter operation and it is equal to the frequency previously defined for the converter operation. After an open-circuit fault, f_s is increased to the double of the original f_s value. In the case of a second open-circuit fault, f_s is subjected to a new increase. In the example illustrated in Figure 4.2, the increase of f_s after fault detection is notorious.

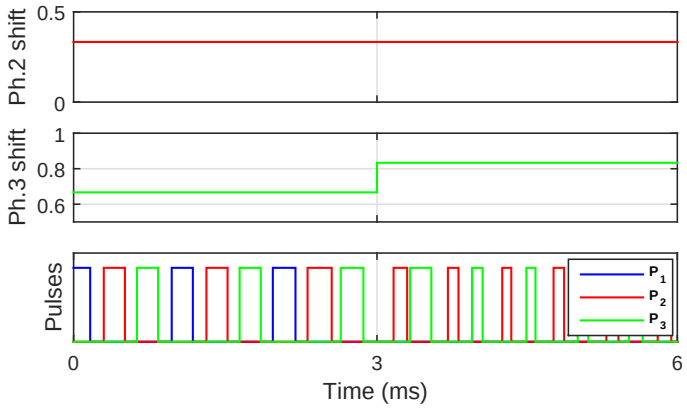

Figure 4.2: PWM reconfiguration after an open-circuit fault in Q1 at $t = 3.1\ ms$.

It should be noted that the use of the reconfiguration strategy, just like in any other converter working under faulty conditions, leads to higher current rates in the healthy power switches that remain operating. This stresses those switches and leads to higher conduction and switching losses, with possible overheating. Converter operation with full load conditions should be, therefore, avoided under these circumstances. Besides that, f_s must be kept inside reasonable limits, taking into account the limitations imposed by the converter inductive components.

Chapter 5

Simulation Results

The solutions proposed in the previous chapters were simulated using MATLAB/Simulink to confirm their effectiveness. The elements and parameters used for simulation purposes were approached as much as possible to the equipment used for experimental purposes.

Figure 5.1 reflects the full system comprising fault detection and reconfiguration.

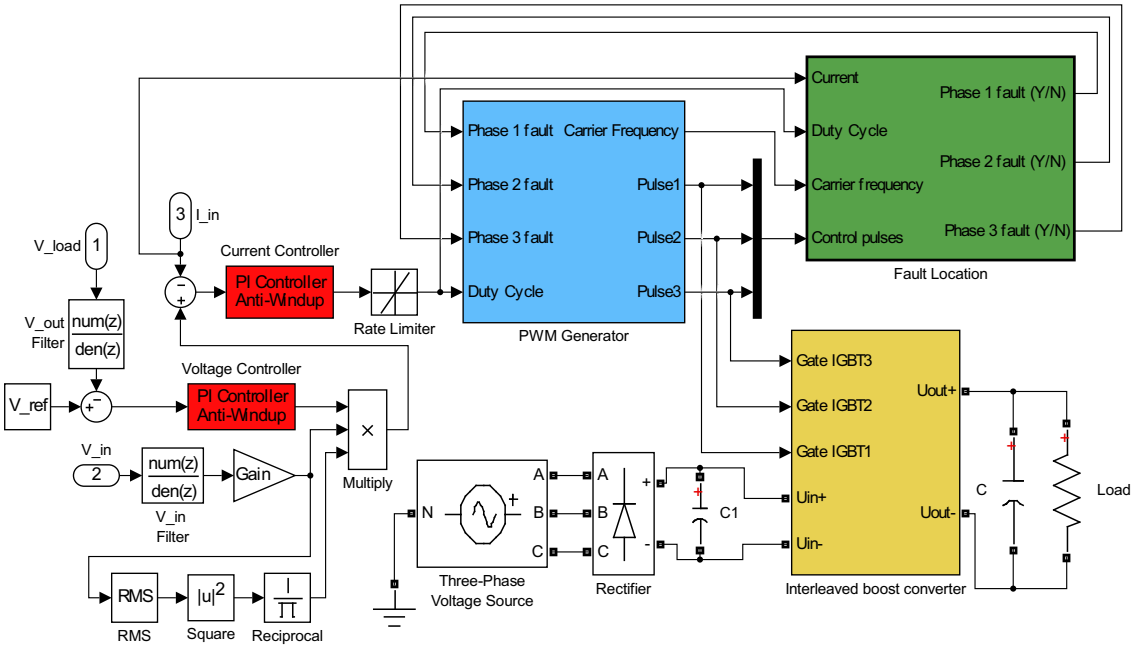

Figure 5.1: Overview of the entire system.

The main parameters used in this simulation are summarized in Tables A.1 to A.5 from Appendix A. Several levels were considered for the converter output voltage V_o, in order to address a wide range of duty cycle D values. A constant resistance load is considered in the tests.

Figures 5.2, 5.3 and 5.4 establish a comparison between the most important converter variables for three different circumstances: in Figure 5.2, no reconfiguration is used after a failure in one of the converter phases; in Figure 5.3, partial reconfiguration is used after a failure, by correcting the phase-shift between healthy phases; and in Figure 5.4, phase-shift correction and frequency modulation are applied after a failure, to get full reconfiguration in the converter. The simulation results presented in these figures were performed for a converter output voltage of $48\ V$.

A comparison study between Figure 5.2 and Figure 5.3 allow us to take some conclusions. A decrease in the ripple has occurred in many of the converter electrical parameters, especially in I_{in}. Despite the fact that phase-shift plays an important role in ripple cancellation after an open-circuit fault, further improvements in the limitation of ripple are attained after combining the increase of f_s with phase-shift correction. Figure 5.4 proves such statement. Under similar circumstances, like those verified in Figures 5.3 and 5.4, the ripple can be reduced with the increase of the f_s to the double of its initial value. An important reduction in the ripple of

I_{Cap} is also verified when the reconfiguration strategies are applied. It is even more important the fact that, after applying full reconfiguration in the converter, it is possible to maintain the levels of ripple in I_{Cap} associated with healthy operation (see Figure 5.4(g)). Besides that, the transient of I_{in} that remains high (see Figure 5.3(a)) is reduced when full reconfiguration is applied (see Figure 5.4(a)). The same conclusions can be taken from Figure 5.5, where I_{in} is depicted with more detail.

The simulation results presented here focused on the converter operation for constant resistive loads. Nevertheless, load fluctuations are also important events that must be taken into account. Therefore, such events should be simulated to attest that false fault detections do not occur. Figure 5.6 depicts the transient verified when one of the two loads initially connected to the converter are unplugged (for $t = 0.5\ s$). Both loads have the same resistance and, hence, I_o decreases to half of its initial value. This transient does not generate false fault detection in any of the converter phases.

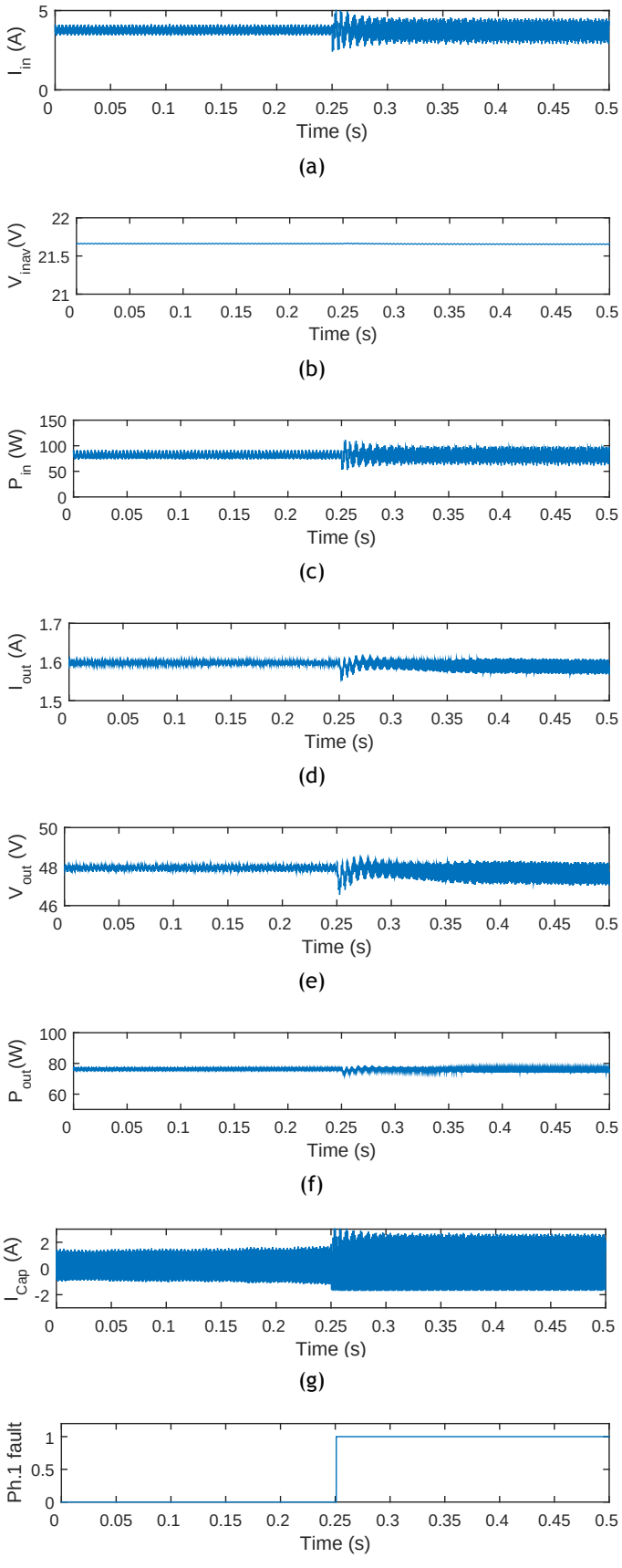

Figure 5.2: Converter variables evolution when an open-circuit fault occurs in one of the converter IGBTs (at $t = 0.25\ s$) and no reconfiguration actions are taken: (a) I_{in}; (b) $V_{in_{av}}$; (c) P_{in}; (d) I_{out}; (e) V_{out}; (f) P_{out}; (g) I_{Cap}; (h) Phase 1 fault detection flag. Switching frequency f_s is equal to $1\ kHz$ and remains unchanged during the simulation.

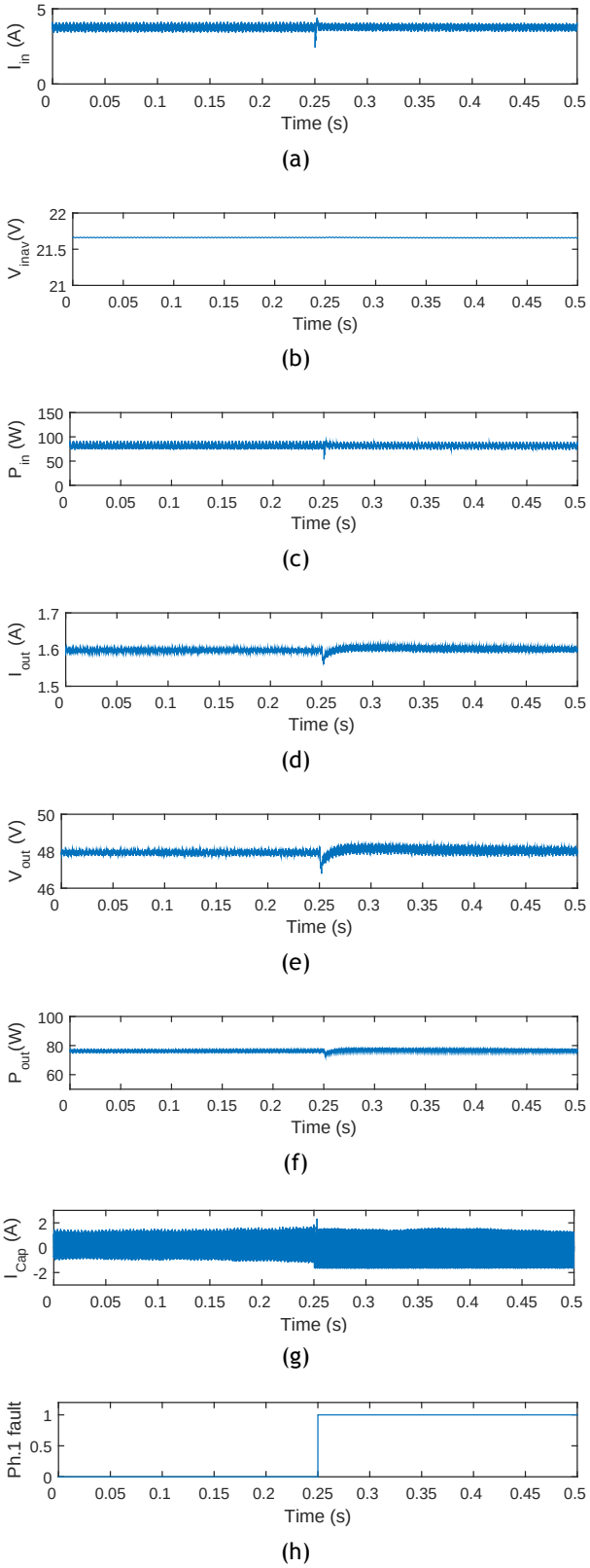

Figure 5.3: Converter variables evolution when an open-circuit fault occurs in one of the converter IGBTs (at $t = 0.25\ s$) and partial reconfiguration actions are taken (only phase-shift is corrected): (a) I_{in}; (b) $V_{in_{av}}$; (c) P_{in}; (d) I_{out}; (e) V_{out}; (f) P_{out}; (g) I_{Cap}; (h) Phase 1 fault detection flag. Switching frequency f_s is equal to $1\ kHz$ and remains unchanged during the simulation.

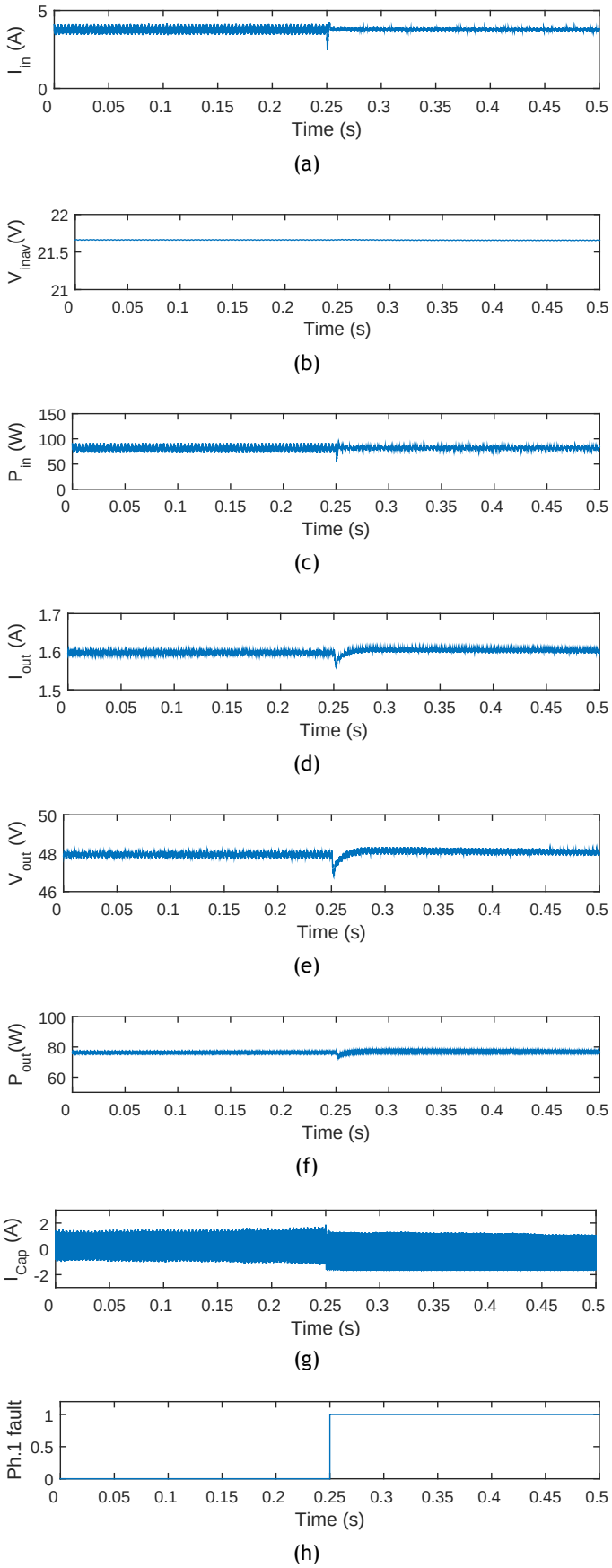

Figure 5.4: Converter variables evolution when an open-circuit fault occurs in one of the converter IGBTs (at $t = 0.25\ s$) and full reconfiguration actions are considered: (a) I_{in}; (b) V_{in}; (c) P_{in}; (d) I_{out}; (e) V_{out}; (f) P_{out};(g) I_{Cap}; (h) Phase 1 fault detection flag. Switching frequency f_s increases from $1\ kHz$ to $2\ kHz$ after detecting the fault.

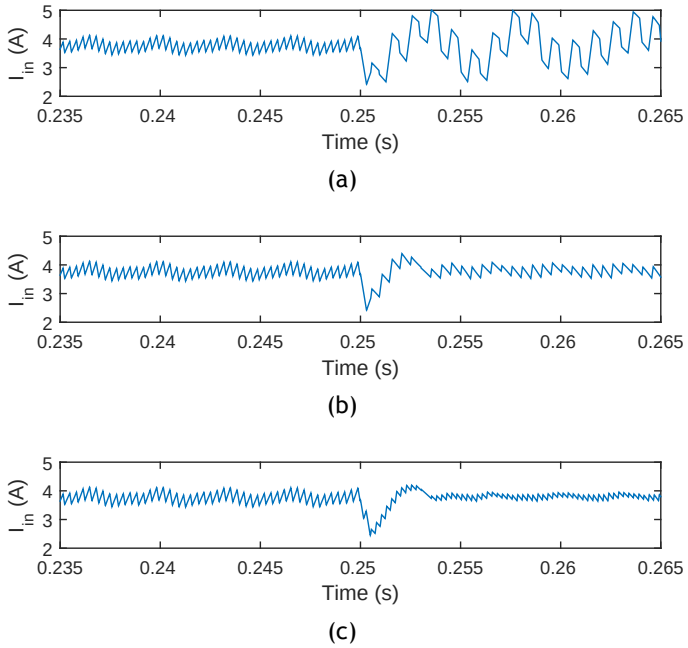

Figure 5.5: Zoom of I_{in}: (a) no reconfiguration strategy is applied to the converter after fault; (b) partial reconfiguration (phase-shift correction) is applied to the converter after fault; (c) full reconfiguration is applied to the converter after a fault detection.

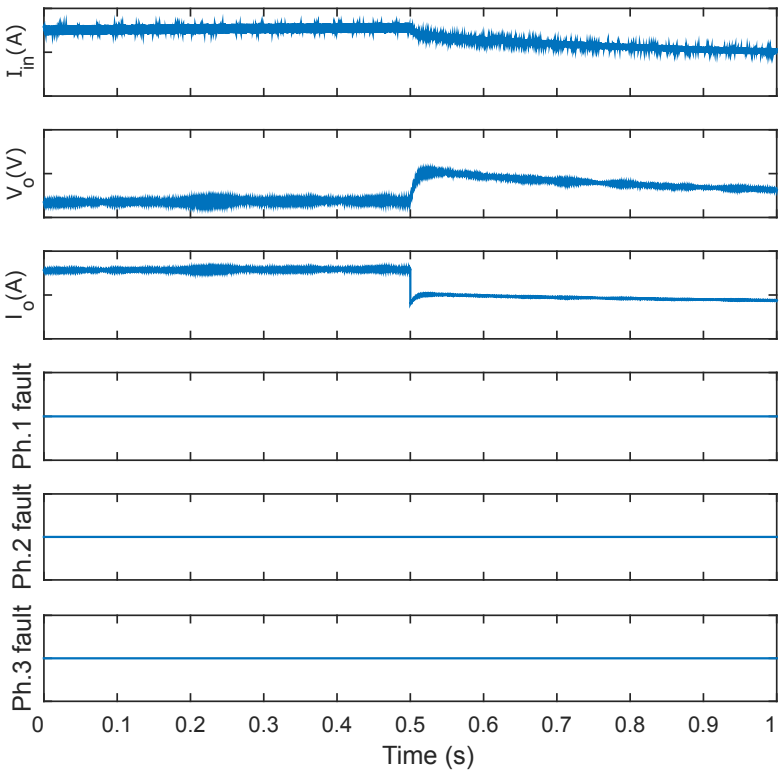

Figure 5.6: Behaviour of the converter most important electrical parameters after a step variation in the load connected to the converter.

Chapter 6

Experimental Set-Up and Results

6.1 Experimental Set-Up

To experimentally verify the proposed method, the converter was connected to a rectifier (see Figure 6.1 and Figure 6.2), in an attempt to mimic a DC plug from a hypothetical system where the DC loads are plugged into DC sockets and the interface between load and grid is made by means of a DC-DC converter. To obtain a stable voltage from the rectifier output, capacitors are connected in parallel with the rectifier output. Most of the parameters used here are equal to the ones specified for the simulation.

The experimental assembly is similar to those used for simulation purposes and comprises:

- One full-bridge diode rectifier
- One capacitor applied to the converter input ($5500\ \mu F$)
- Three inductances ($7.6\ mH$)
- Three IGBTs and diodes
- One capacitor for the converter output ($680\ \mu F$)
- One programmable DC electronic load
- Digital controller dSPACE DS1103

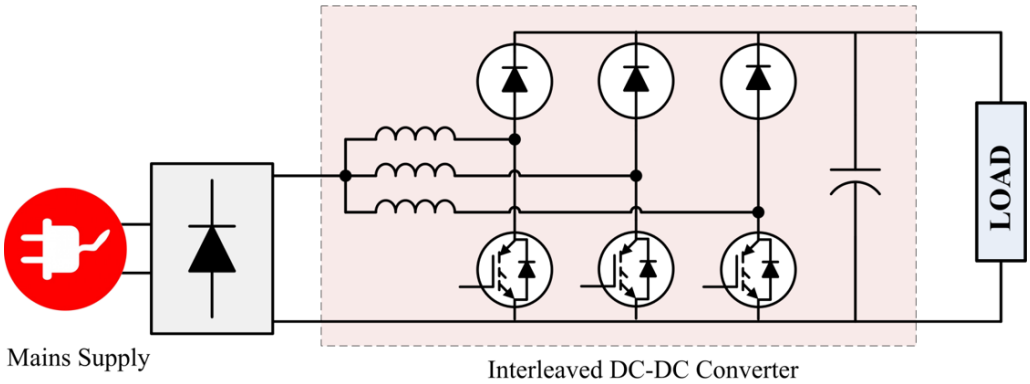

Figure 6.1: Scheme of the experimental set-up (symbolic).

To control the converter, the input current I_{in}, the input voltage V_{in} and the output voltage V_o are measured and introduced in dSPACE. Other measurements are taken too, but only for safety purposes.

The electronic load operates under constant resistance condition, with a resistor of $30\ \Omega$. Some load variations were also applied in the experimental set-up to prove the results obtained for the simulation with load variation.

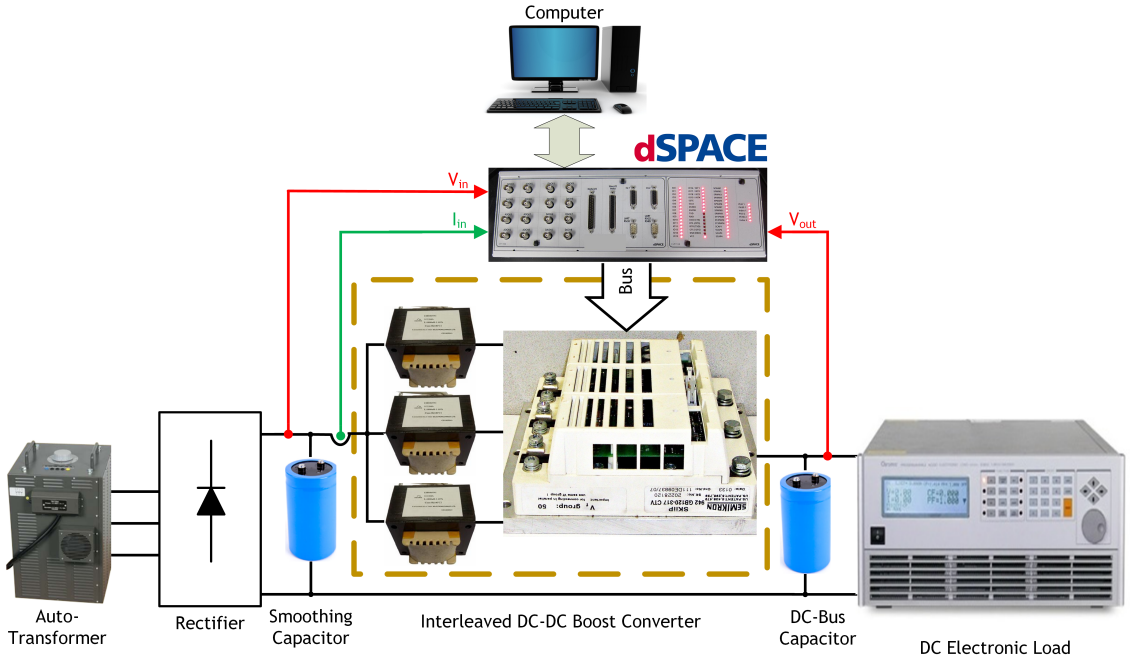

Figure 6.2: Scheme of the experimental set-up (physical).

The digital controller operates with a sampling time of $15\ \mu s$; the converter initially operates with a switching frequency f_s of $1\ kHz$. To force an open-circuit fault in any of the IGBTs, the desired PWM signal(s) are turned on and off using the dSPACE ControlDesk software.

6.2 Experimental Results

Experimental data are shown in Figures 6.3, 6.4 and 6.5. An open-circuit fault is introduced in IGBT Q1 (see Figure 2.1) at $t = 0.25\ s$. Under these conditions, the fault is detected after $0.53\ ms$, corresponding to a few more than half of a switching period, which is reasonable for the conditions under analysis. In Figure 6.3, no reconfiguration is applied. An increase in the ripple of I_{in} is observed, as one of the converter phases stopped working and the remaining phases still behave like they were working in a three-phase converter. Hence, the ripple in the current flowing through the output capacitor also increases, in an attempt to stabilize the current provided to the load. A slight increase in the ripple of I_{out} and other parameters from the converter output is also verified, but in a lesser extent when compared with the ripple increase of I_{in}. In Figure 6.4, data related with converter partial reconfiguration is presented. Comparing with pre-fault conditions, slightly higher levels of ripple are verified after a fault when only phase correction is used. Finally, Figure 6.5 depicts the evolution of the same variables when the proposed reconfiguration strategy is applied. After detecting the fault, the phase correction block changes to $\pi\ rad$ the phase shift between pulses related with IGBTs whose operation remains intact and, at the same time, it raises the frequency of those pulses to $2\ kHz$. Ripple levels are reduced even more and the spike verified in the fault moment is slightly alleviated.

Figure 6.6 gives a zoomed view of I_{in} for the three situations under study. When no reconfiguration is applied, I_{in} ripple approaches $1\ A$, which represents almost $1/3$ of the total converter input current. Meanwhile, the reconfiguration reduces the ripple of I_{in} to almost $0.3\ A$, that represents $1/10$ of the total converter input current and ripple values even lower to those verified before the fault. This fact has a feasible explanation. Under normal circumstances, the

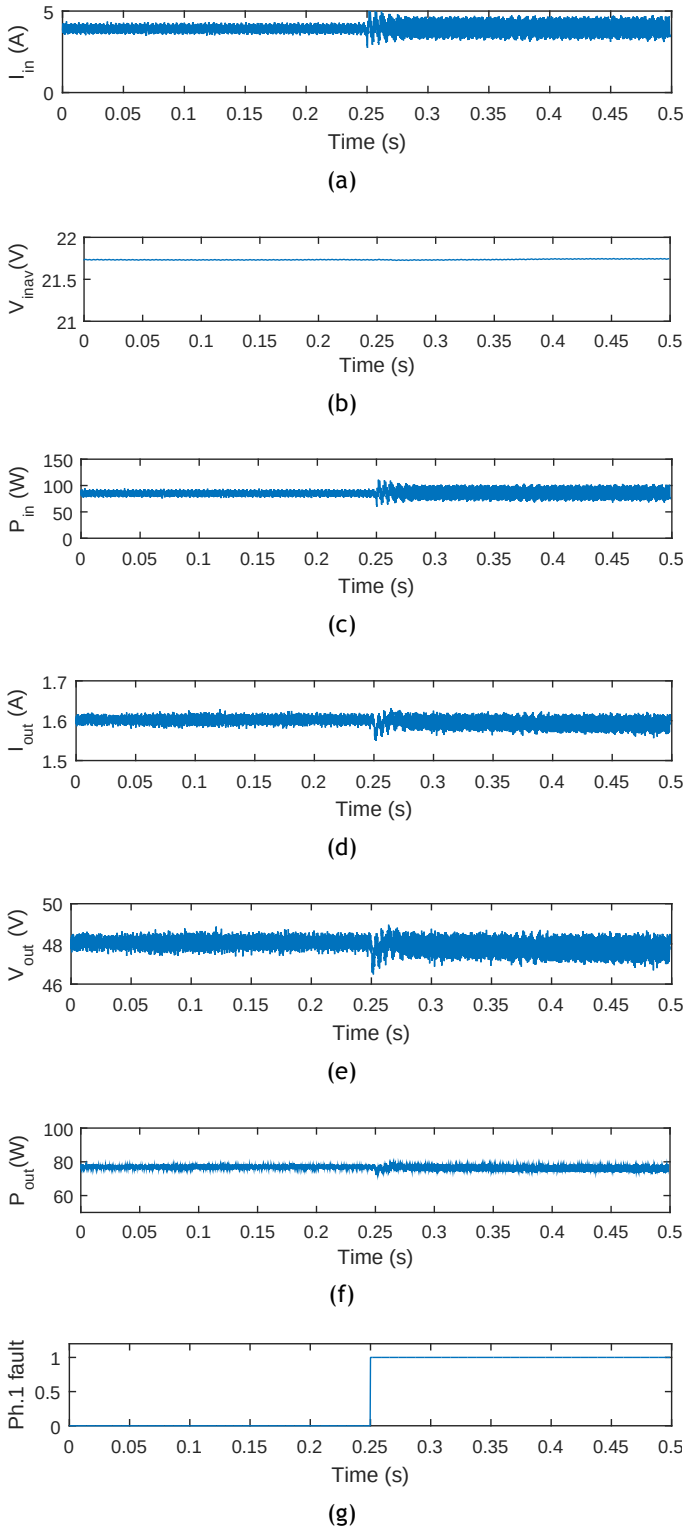

Figure 6.3: Converter variables evolution when an open-circuit fault occurs in one of the converter phases: (a) I_{in}; (b) $V_{in_{av}}$; (c) P_{in}; (d) I_{out}; (e) V_{out}; (f) P_{out}; (g) Phase 1 fault detection flag. Switching frequency f_s is equal to $1\ kHz$ and remains unchanged during the experiment.

converter operates with f_s equal to $1\ kHz$ and three phases. Hence, I_{in} ripple frequency will be equal to $N \times f_s = 3 \times 1000 = 3000\ Hz = 3\ kHz$. After an open-circuit fault, the converter controller imposes a switching frequency f_s equal to $2\ kHz$. As the number of healthy phases has reduced to two, I_{in} ripple frequency will be equal to $N \times f_s = 2 \times 2000 = 4000\ Hz = 4\ kHz$.

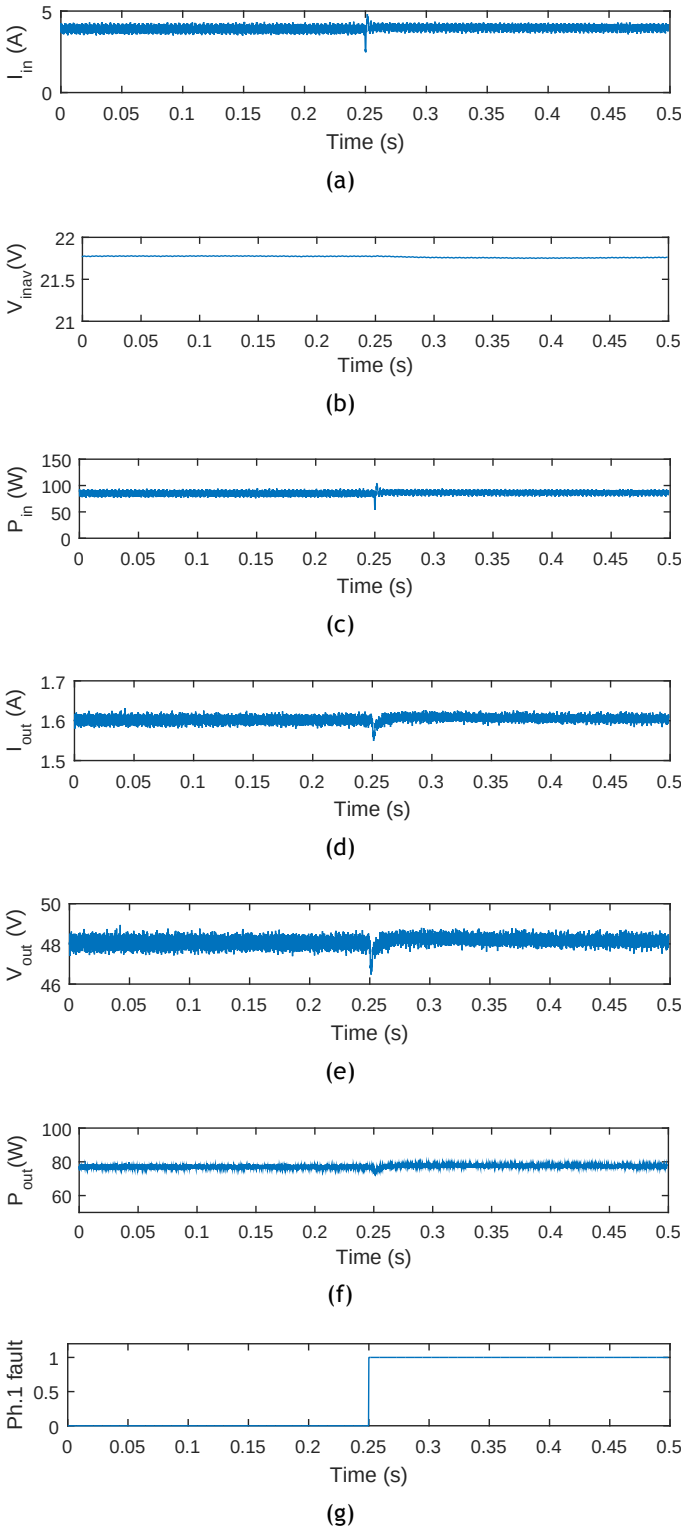

Figure 6.4: Converter variables evolution when phase-shift correction is applied after an open-circuit fault: (a) I_{in}; (b) $V_{in_{av}}$; (b) P_{in}; (d) I_{out}; (e) V_{out}; (f) P_{out}; (g) Phase 1 fault detection flag. Switching frequency f_s is equal to $1\ kHz$ and remains unchanged during the experiment.

Therefore, an increase in the frequency of the I_{in} ripple is actually achieved, contributing in a curtailment in the I_{in} ripple amplitude.

Another important datum is the good performance of the converter in terms of efficiency, even after an open-circuit fault. When the converter operates under normal conditions, the

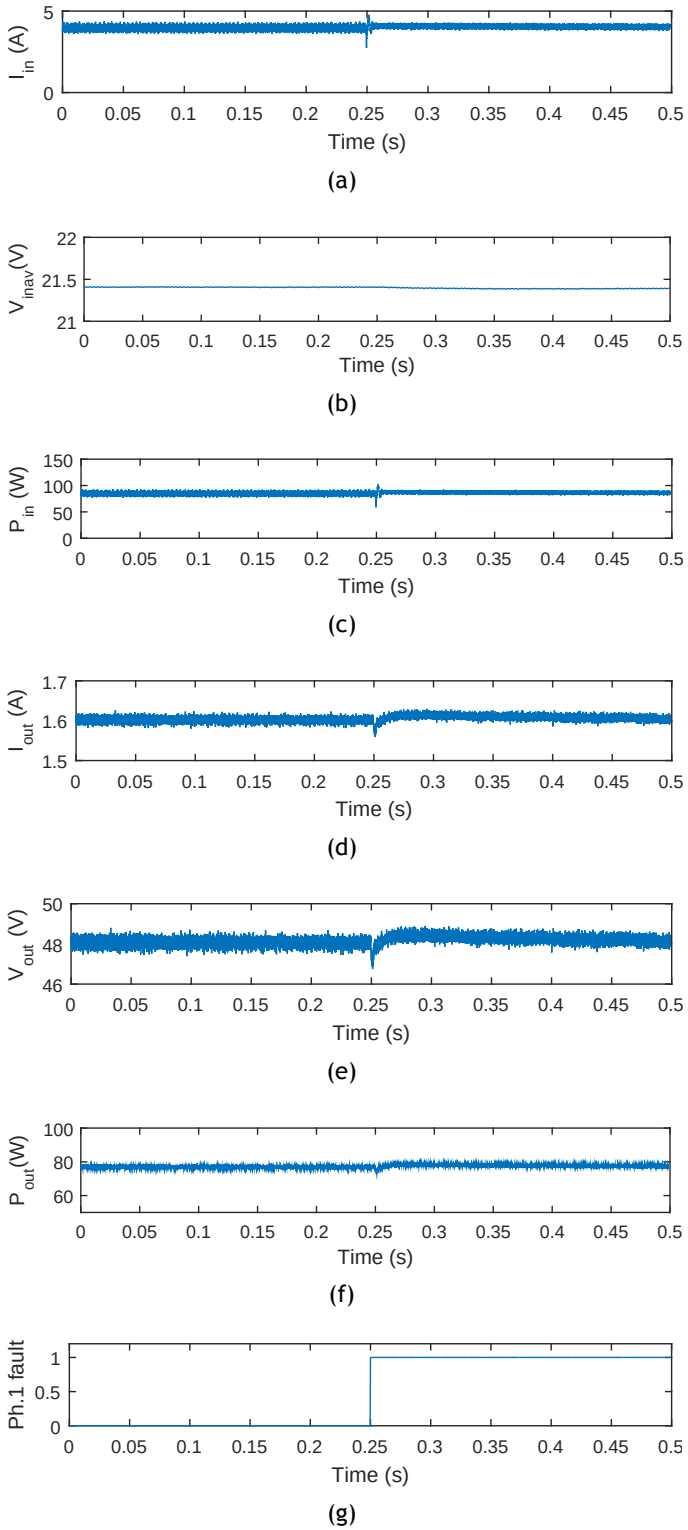

Figure 6.5: Converter variables evolution when full reconfiguration is applied after fault detection: (a) I_{in}; (b) $V_{in_{av}}$; (c) P_{in}; (d) I_{out}; (e) V_{out}; (f) P_{out}; (g) Phase 1 fault detection flag. Switching frequency f_s increases from $1\ kHz$ to $2\ kHz$ after detecting the fault.

efficiency of the converter rounds 90%. After a fault, the converter efficiency remains almost unchanged. This is an important indicator of the reconfiguration strategy, as it does not significantly impact the converter efficiency.

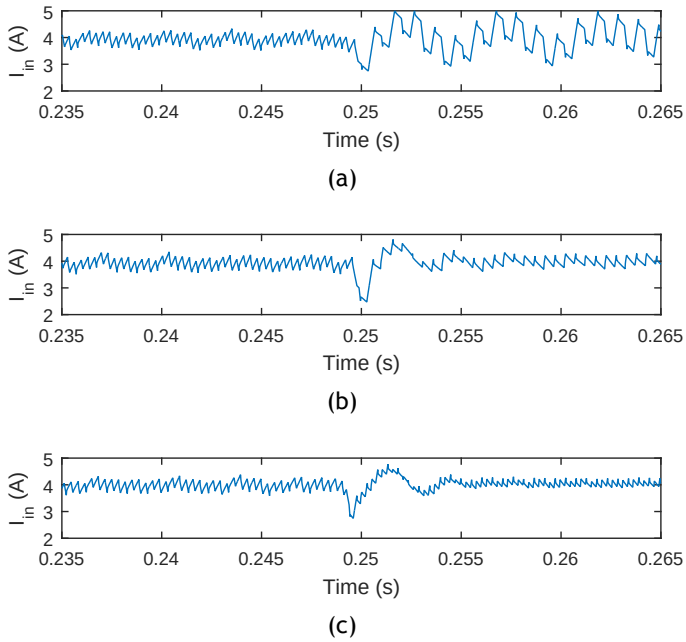

Figure 6.6: Detail of I_{in}: (a) no reconfiguration strategy is applied to the converter after fault; (b) only phase-shift is corrected after a fault detection; (c) full reconfiguration is applied.

Chapter 7

Conclusions and Suggestions for Future Works

7.1 Conclusions

The use of DC-DC converters is gaining importance. Until now, DC-DC converters were mainly dedicated to industrial applications. However, these converters may become part of our home appliances soon, as concerns about our dwelling's energy efficiency increases. Many of our home appliances require power converters with high reliability levels, in order to extend the lifespan of those appliances. These converters, like any other converter, may suffer faults that degrade their smooth operation, compromising the converters themselves as well as the load connected to them, reducing their lifespan. Locating the sources of these faults to take remedial actions that minimize their effects present, therefore, great importance.

This dissertation presented fault detection and fault reconfiguration strategies applied to open-circuit faults in the power switches of a multi-phase DC-DC converter. Regardless of that, these strategies can be used for many other DC-DC converter topologies either.

As expected, the experimental results meet pretty well the expected behaviour, with coincident results in both simulation and experimental essays.

Phase-shift correction was the most common reconfiguration strategy used in previous works focused on fault-tolerant multi-phase converters. On the other hand, variable frequency drivers used in the literature were mainly focused on other purposes than the fault tolerance. This work showed that both techniques are effective when applied in fault-tolerant converters. Besides that, it was shown that the combination of several reconfiguration techniques leads to improved results, not achieved in fault tolerant converters that make use of just one reconfiguration strategy, and great benefits are achieved in the operation of faulty DC-DC converters, enabling the continued operation of the converter, without any redundant components.

7.2 Suggestions for Future Works

Taking into account the work developed in the dissertation and an improved knowledge about the DC-DC converters subject, some suggestions can be proposed for future works in this area, with a great potential to grow up.

- Increase the efficiency and power density of the power converters, with special focus to the devices with large step in voltage, which will be essential for the DC grids deployment;
- Deploy power converters that take advantage from Wide Bandgap semiconductors, taking into account the particularities of these devices;
- Investigate/develop new fault detection and avoidance/tolerance techniques with a broad range of action and quick response to faults.

Bibliography

[1] P. Bertoldi, N. Labanca, B. Hirl, European Commission, Joint Research Centre, and Institute for Energy and Transport., *Energy efficiency status report 2012 electricity consumption and efficiency trends in the EU - 27*. Luxembourg: Publications Office, 2012. [Online]. Available: http://dx.publications.europa.eu/10.2788/37564

[2] Energy appliances monitoring - ENEA. [Accessed: 17 May 2016]. [Online]. Available: http://www.enea.it/it/laboratori-di-ricerca-di-ispra/documenti/eventi/Energyappliancesmonitoring_ENEAPistochini.pdf

[3] D. Bosseboeuf, L. Gynther, B. Lapillonne, and K. Pollier. (2015) Energy Efficiency Trends and Policies in the Household and Tertiary Sectors. [Accessed: 3 May 2016]. [Online]. Available: http://www.odyssee-mure.eu/publications/br/energy-efficiency-in-buildings.html

[4] Electronic speed regulator. [Accessed: 15 April 2016]. [Online]. Available: http://paginas.fe.up.pt/~ee95203/pass_macho.htm

[5] Mini Split Buying Guide: How to Pick the Perfect Mini Split. [Accessed: 14 April 2016]. [Online]. Available: http://www.ecomfort.com/stories/1184-How-to-Pick-the-Perfect-Mini-Split.html

[6] C. C. Chan and K. T. Chau, "An overview of power electronics in electric vehicles," *IEEE Transactions on Industrial Electronics*, vol. 44, no. 1, pp. 3–13, Feb 1997.

[7] M. Davis, "Energy efficiency policies and measures in Portugal / ODYSSEE-MURE 2010," Jun. 2013. [Online]. Available: http://www.buildup.eu/en/practices/publications/energy-efficiency-policies-and-measures-portugal-odyssee-mure-2010

[8] FuturEnergy 1kW Turbine Technical Specifications. [Accessed: 13 May 2016]. [Online]. Available: http://www.futurenergy.co.uk/turbine.html

[9] I. Staffell, D. J. L. Brett, N. P. Brandon, and A. D. Hawkes, *Domestic Microgeneration: Renewable and Distributed Energy Technologies, Policies and Economics*. Routledge, June 2015.

[10] B. Singh, S. Singh, A. Chandra, and K. Al-Haddad, "Comprehensive Study of Single-Phase AC-DC Power Factor Corrected Converters With High-Frequency Isolation," *IEEE Transactions on Industrial Informatics*, vol. 7, no. 4, pp. 540–556, Nov 2011.

[11] B. Patterson. (2015) DC Power Distribution Systems. [Accessed: 5 May 2016]. [Online]. Available: http://tinyurl.com/jr66sw7

[12] H. Kakigano, M. Nomura, and T. Ise, "Loss evaluation of DC distribution for residential houses compared with AC system," in *2010 International Power Electronics Conference*, June 2010, pp. 480–486.

[13] G. S. Seo, J. Baek, K. Choi, H. Bae, and B. Cho, "Modeling and analysis of DC distribution systems," in *2011 IEEE 8th International Conference on Power Electronics and ECCE Asia*, May 2011, pp. 223–227.

[14] V.-J. Webb, "Design of a 380 V/24 V DC micro-grid for residential DC distribution," Ph.D. dissertation, The University of Toledo, 2013.

[15] V. Vossos, K. Garbesi, and H. Shen, "Energy savings from direct-dc in u.s. residential buildings," *Energy and Buildings*, vol. 68, Part A, pp. 223 – 231, 2014. [Online]. Available: http://www.sciencedirect.com/science/article/pii/S0378778813005720

[16] DC in the Home. [Accessed: 10 May 2016]. [Online]. Available: https://standards.ieee.org/email/2013_10_cfp_dchome_web.html

[17] India Low Voltage DC Forum. [Accessed: 10 May 2016]. [Online]. Available: http://standards.ieee.org/news/2014/LVDC_forum.html

[18] Z. J. Shen, Z. Miao, and A. M. Roshandeh, "Solid state circuit breakers for DC micrgrids: Current status and future trends," in *2015 IEEE First International Conference on DC Microgrids*, June 2015, pp. 228–233.

[19] Y. Bingjian, G. Yang, W. Xiaoguang, H. Zhiyuan, C. Longlong, and S. Yunhai, "A hybrid circuit breaker for DC-application," in *2015 IEEE First International Conference on DC Microgrids*, June 2015, pp. 187–192.

[20] H. Matsuo, S. Matsumoto, M. Suetomi, S. Fujino, K. Harada, W. Lin, and Y. Sui, "Novel DC switch and DC socket for high voltage DC power feeding systems," in *2012 IEEE 34th International Telecommunications Energy Conference*, Sept 2012, pp. 1–4.

[21] K. Tan, A. Q. Huang, and A. Martin, "Development of solid state arc-free socket for DC distribution system," in *2014 IEEE Applied Power Electronics Conference and Exposition*, March 2014, pp. 2300–2305.

[22] T. Yuba, S. Baek, K. Kiryu, A. Nakamura, H. Miyazawa, M. Noritake, and K. Hirose, "Development of plug and socket-outlet for 400 volts direct current distribution system," in *2011 IEEE 8th International Conference on Power Electronics and ECCE Asia*, May 2011, pp. 218–222.

[23] Wide Bandgap Semiconductors: Pursuing the Promise. [Accessed: 16 May 2016]. [Online]. Available: https://www1.eere.energy.gov/manufacturing/rd/pdfs/wide_bandgap_semiconductors_factsheet.pdf

[24] J. Millán, P. Godignon, X. Perpiñà, A. Pérez-Tomás, and J. Rebollo, "A survey of wide bandgap power semiconductor devices," *IEEE Transactions on Power Electronics*, vol. 29, no. 5, pp. 2155–2163, May 2014.

[25] S. Saksena and S. G. Karady, "Effects of voltage sags on household loads," in *IEEE Power Engineering Society General Meeting, 2005*, June 2005, pp. 2456–2461 Vol. 3.

[26] M. C. L. Yong and P. Yin, "Effects voltage sag on single-phase domestic and office loads," *Electrical Power Quality & Utilization Magazine*, vol. 4, no. 1, Sept 2009.

[27] E. N. Power, "Effects of AC ripple current on VRLA battery life," *A Technical Note from the Experts in Business-Critical Continuity*, 2010.

[28] K. Zhao, P. Ciufo, and S. Perera, "Rectifier Capacitor Filter Stress Analysis When Subject to Regular Voltage Fluctuations," *IEEE Transactions on Power Electronics*, vol. 28, no. 7, pp. 3627–3635, July 2013.

[29] A. Khosroshahi, M. Abapour, and M. Sabahi, "Reliability Evaluation of Conventional and Interleaved DC–DC Boost Converters," *IEEE Transactions on Power Electronics*, vol. 30, no. 10, pp. 5821–5828, Oct 2015.

[30] C. Brunson, L. Empringham, L. D. Lillo, P. Wheeler, and J. Clare, "Open-Circuit Fault Detection and Diagnosis in Matrix Converters," *IEEE Transactions on Power Electronics*, vol. 30, no. 5, pp. 2840–2847, May 2015.

[31] S. Yang, A. Bryant, P. Mawby, D. Xiang, L. Ran, and P. Tavner, "An Industry-Based Survey of Reliability in Power Electronic Converters," *IEEE Transactions on Industry Applications*, vol. 47, no. 3, pp. 1441–1451, May 2011.

[32] X. Pei, S. Nie, and Y. Kang, "Switch Short-Circuit Fault Diagnosis and Remedial Strategy for Full-Bridge DC–DC Converters," *IEEE Transactions on Power Electronics*, vol. 30, no. 2, pp. 996–1004, Feb 2015.

[33] E. Jamshidpour, P. Poure, and S. Saadate, "Photovoltaic Systems Reliability Improvement by Real-Time FPGA-Based Switch Failure Diagnosis and Fault-Tolerant DC–DC Converter," *IEEE Transactions on Industrial Electronics*, vol. 62, no. 11, pp. 7247–7255, Nov 2015.

[34] M. Gleissner and M. M. Bakran, "Design and Control of Fault-Tolerant Nonisolated Multiphase Multilevel DC–DC Converters for Automotive Power Systems," *IEEE Transactions on Industry Applications*, vol. 52, no. 2, pp. 1785–1795, March 2016.

[35] F. Deng, Z. Chen, M. R. Khan, and R. Zhu, "Fault Detection and Localization Method for Modular Multilevel Converters," *IEEE Transactions on Power Electronics*, vol. 30, no. 5, pp. 2721–2732, May 2015.

[36] X. Pei, S. Nie, Y. Chen, and Y. Kang, "Open-Circuit Fault Diagnosis and Fault-Tolerant Strategies for Full-Bridge DC–DC Converters," *IEEE Transactions on Power Electronics*, vol. 27, no. 5, pp. 2550–2565, May 2012.

[37] K. Park and Z. Chen, "Open-circuit fault detection and tolerant operation for a parallel-connected SAB DC-DC converter," in *2014 Twenty-Ninth Annual IEEE Applied Power Electronics Conference and Exposition*, March 2014, pp. 1966–1972.

[38] E. Ribeiro, A. J. M. Cardoso, and C. Boccaletti, "Open-Circuit Fault Diagnosis in Interleaved DC–DC Converters," *IEEE Transactions on Power Electronics*, vol. 29, no. 6, pp. 3091–3102, June 2014.

[39] T. Kamel, Y. Biletskiy, and L. Chang, "Real-Time Diagnosis for Open-Circuited and Unbalance Faults in Electronic Converters Connected to Residential Wind Systems," *IEEE Transactions on Industrial Electronics*, vol. 63, no. 3, pp. 1781–1792, March 2016.

[40] A. Ghazanfari and Y. A. R. I. Mohamed, "A Resilient Framework for Fault-Tolerant Operation of Modular Multilevel Converters," *IEEE Transactions on Industrial Electronics*, vol. 63, no. 5, pp. 2669–2678, May 2016.

[41] E. Ribeiro, A. J. M. Cardoso, and C. Boccaletti, "Fault diagnosis in unidirectional non-isolated DC-DC converters," in *2014 IEEE Energy Conversion Congress and Exposition*, Sept 2014, pp. 1140–1145.

[42] E. Ribeiro, A. J. M. Cardoso, and C. Boccaletti, "Fault-Tolerant Strategy for a Photovoltaic DC–DC Converter," *IEEE Transactions on Power Electronics*, vol. 28, no. 6, pp. 3008–3018, June 2013.

[43] H. Sheng, F. Wang, and C. W. Tipton IV, "A Fault Detection and Protection Scheme for Three-Level DC–DC Converters Based on Monitoring Flying Capacitor Voltage," *IEEE Transactions on Power Electronics*, vol. 27, no. 2, pp. 685–697, Feb 2012.

[44] Y. Chen, X. Pei, S. Nie, and Y. Kang, "Monitoring and Diagnosis for the DC–DC Converter Using the Magnetic Near Field Waveform," *IEEE Transactions on Industrial Electronics*, vol. 58, no. 5, pp. 1634–1647, May 2011.

[45] J. Poon, P. Jain, I. Konstantakopoulos, C. Spanos, S. Panda, and S. Sanders, "Model-Based Fault Detection and Identification for Switching Power Converters," *IEEE Transactions on Power Electronics*, 2016, Early Access.

[46] S. Nie, X. Pei, Y. Chen, and Y. Kang, "Fault Diagnosis of PWM DC–DC Converters Based on Magnetic Component Voltages Equation," *IEEE Transactions on Power Electronics*, vol. 29, no. 9, pp. 4978–4988, Sept 2014.

[47] D. H. Kim, G. Y. Choe, and B. K. Lee, "DCM Analysis and Inductance Design Method of Interleaved Boost Converters," *IEEE Transactions on Power Electronics*, vol. 28, no. 10, pp. 4700–4711, Oct 2013.

[48] N. Genc and I. Iskender, "DSP-based current sharing of average current controlled two-cell interleaved boost power factor correction converter," *IET Power Electronics*, vol. 4, no. 9, pp. 1015–1022, November 2011.

[49] B. Sun, "Digital current balancing for an interleaved boost PFC," *Analog Applications*, 2013.

[50] L. Dixon, "Average current mode control of switching power supplies," in *Unitrode Power Supply Design Seminar Manual SEM700*, Feb 1990, pp. 1–12.

[51] L. Ni, D. J. Patterson, and J. L. Hudgins, "High Power Current Sensorless Bidirectional 16-Phase Interleaved DC-DC Converter for Hybrid Vehicle Application," *IEEE Transactions on Power Electronics*, vol. 27, no. 3, pp. 1141–1151, March 2012.

[52] N. Težak and M. Macan, "Adaptive PWM control scheme of interleaved boost converter for AC traction application," in *2010 14th International Power Electronics and Motion Control Conference*, Sept 2010, pp. T9–72–T9–77.

[53] A. Vazquez, M. Arias, A. Rodriguez, D. G. Lamar, and S. Luri, "Master-slave technique with direct variable frequency control for interleaved bidirectional boost converter," in *2014 IEEE Energy Conversion Congress and Exposition*, Sept 2014, pp. 956–963.

[54] D.-M. Joo, D.-H. Kim, and B.-K. Lee, "DCM Frequency Control Algorithm for Multi-Phase DC-DC Boost Converters for Input Current Ripple Reduction," *Journal of Electrical Engineering & Technology*, vol. 10, no. 6, pp. 2307–2314, 2015.

[55] Q. Li and P. Wolfs, "An Analysis of the ZVS Two-Inductor Boost Converter under Variable Frequency Operation," *IEEE Transactions on Power Electronics*, vol. 22, no. 1, pp. 120–131, Jan 2007.

Appendix A

Simulation Parameters

In order to approach the simulation as much as possible to the experimental set-up, the following parameters were defined.

Table A.1: Converter parameters.

Inductance (L_i)	$7.6\ mH$
Input capacitance (C_{in})	$5500\ \mu F$
Output capacitance (C_o)	$680\ \mu F$

Table A.2: Converter diodes parameters.

R_{on}	$5.7\ m\Omega$
L_{on}	$0\ H$
Forward voltage V_f	$0.7\ V$
Snubber resistance R_s	$3500\ \Omega$
Snubber capacitance C_s	inf

Table A.3: Converter IGBTs parameters.

R_{on}	$14.7\ m\Omega$
L_{on}	$0\ H$
Forward voltage V_f	$1.2\ V$
T_f	$1\ \mu s$
T_t	$2\ \mu s$
Snubber resistance R_s	$100\ k\Omega$
Snubber capacitance C_s	inf

Table A.4: Current controller parameters.

D Rising slew rate	100
D Falling slew rate	-100
PI Voltage controller K_p	0.015
PI Voltage controller K_i	0.2
PI Current controller K_p	0.5
PI Current controller K_i	0.8
Gain	1/70

Table A.5: Load and other control parameters.

Load resistance	$30\ \Omega$
Switching frequency	$1\ kHz$
Sampling time	$5\ \mu s$

Glossary

BCM	DC-DC converter operation mode in which the current flowing through the converter inductances reaches zero in a single moment per period.
CCM	DC-DC converter operation mode in which the current flowing through the converter inductances never reaches zero.
DCM	DC-DC converter operation mode in which the current flowing through the converter inductances temporarily reaches zero in every switching period.